

**Negative Regulation of Human Hepatic Constitutive Androstane Receptor by Cholesterol  
Synthesis Inhibition: Role of Sterol Regulatory Element Binding Proteins**

Liberta Cuko, Zofia Duniec-Dmuchowski, Elizabeth A. Rondini<sup>1</sup>, Asmita Pant<sup>2</sup>, John K. Fallon,  
Elizabeth M. Wilson<sup>3</sup>, Nicholas J. Peraino, Judy A. Westrick, Philip C. Smith, and Thomas A.  
Kocarek

Institute of Environmental Health Sciences (L.C., Z. D.-D., E.A.R., A.P., T.A.K.) and Department  
of Chemistry (N.J.P., J.A.W.), Wayne State University, Detroit, MI; Yecuris Corporation,  
Tualatin, OR (E.M.W.); and Division of Pharmacoengineering and Molecular Pharmaceutics,  
University of North Carolina, Chapel Hill, NC (J.K.F., P.C.S.).

**Running Title:** Human CAR regulation by cholesterol synthesis inhibition

**Address correspondence to:** Dr. Thomas Kocarek, Institute of Environmental Health Sciences, 6135 Woodward Ave, Room 2126, Wayne State University, Detroit, MI 48202, USA.  
Tel: (313) 577-6580; FAX: (313) 972-8025; E-mail: t.kocarek@wayne.edu

Number of text pages: 48

Number of tables: 3 supplemental

Number of figures: 9 and 3 supplemental

Number of references: 54

Number of words in Abstract: 247

Number of words in Introduction: 756

Number of words in Discussion: 1504

**Abbreviations:** ANOVA, analysis of variance; BSA, bovine serum albumin; CAR, constitutive androstane receptor or NR1I3; CITCO, 6-(4-chlorophenyl)imidazo[2,1-b][1,3]thiazole-5-carbaldehyde O-(3,4-dichlorobenzyl)oxime; DMSO, dimethyl sulfoxide; FBS, fetal bovine serum; FPP, farnesyl pyrophosphate; FXR, farnesoid X receptor or NR1H4; HMGCR, 3-hydroxy-3-methylglutaryl coenzyme A reductase; HNF4 $\alpha$ , hepatocyte nuclear factor 4 alpha; LC, liquid chromatography; MCT, multiple comparison test; MRM, multiple reaction monitoring; MS, mass spectrometry; MVA, mevalonate; P450, cytochrome P450; PB, phenobarbital; PGC1 $\alpha$ , PPARG coactivator 1 alpha; POR, cytochrome P450 oxidoreductase; Prava, pravastatin; PXR, pregnane X receptor or NR1I2; Rif, rifampicin; RT-qPCR, reverse transcription-quantitative polymerase chain reaction; shCAR, short hairpin RNA targeting human CAR; shNT, non-targeting short hairpin RNA; shRNA, short hairpin RNA; SIL, stable isotope labeled; SPE, solid phase

extraction; Squal1, squalenstatin 1; SREBP1a, sterol regulatory element binding protein 1a;  
SREBP1c, sterol regulatory element binding protein 1c; SREBP2, sterol regulatory element  
binding protein 2; SREBF1, sterol regulatory element binding transcription factor 1; SREBF2,  
sterol regulatory element binding transcription factor 2

## Abstract

The squalene synthase inhibitor squalenyl acetate 1 (Squal1) is a potent and efficacious inducer of CYP2B expression in primary cultured rat hepatocytes and rat liver. To determine whether Squal1 is also an inducer of human CYP2B, the effects of Squal1 treatment were evaluated in primary cultured human hepatocytes, differentiated HepaRG cells, and humanized mouse livers. Squal1 treatment did not increase CYP2B6 mRNA levels in human hepatocytes or HepaRG cells and only slightly and inconsistently increased CYP2B6 mRNA content in humanized mouse liver. However, treatment with farnesol, which mediates Squal1's effect on rat CYP2B expression, increased CYP2B6 mRNA levels in HepaRG cells expressing the constitutive androstane receptor (CAR) but not in cells with knocked-down CAR. To determine the impact of cholesterol biosynthesis inhibition on CAR activation, the effects of pravastatin (Prava) were determined on CITCO-mediated gene expression in primary cultured human hepatocytes. Prava treatment abolished CITCO-inducible CYP2B6 expression, but had less effect on rifampicin-mediated CYP3A4 induction, and CITCO treatment did not affect Prava-inducible HMG-CoA reductase (HMGCR) expression. Treatment with inhibitors of different steps of cholesterol biosynthesis attenuated CITCO-mediated CYP2B6 induction in HepaRG cells, and Prava treatment increased HMGCR expression and inhibited CYP2B6 induction with comparable potency. Transfection of HepG2 cells with transcriptionally active sterol responsive element binding proteins (SREBPs) reduced CAR-mediated transactivation, and inducible expression of transcriptionally active SREBP2 attenuated CITCO-inducible CYP2B6 expression in HepaRG cells. These findings suggest that Squal1 does not induce CYP2B6 in human hepatocytes because Squal1's inhibitory effect on cholesterol biosynthesis interferes with CAR activation.

**Significance Statement:** The cholesterol biosynthesis inhibitor squalestatin 1 induces rat hepatic CYP2B expression indirectly, by causing accumulation of an endogenous isoprenoid that activates the constitutive androstane receptor (CAR). This study demonstrates that squalestatin 1 does not similarly induce CYP2B6 expression in human hepatocytes. Rather, inhibition of cholesterol biosynthesis interferes with CAR activity, likely by activating sterol regulatory element binding proteins. These findings increase our understanding of the endogenous processes that modulate human drug-metabolizing gene expression.

## Introduction

The xenobiotic-sensing receptors pregnane X receptor (PXR, NR1I2) and constitutive androstane receptor (CAR, NR1I3) respond to the presence of a variety of foreign chemicals by transducing their detection into transcriptional regulation of target genes (Wang et al., 2012). While PXR is activated by direct binding of agonists to a large and expansile ligand-binding pocket (Watkins et al., 2003), most CAR activators, including the prototype phenobarbital (PB), do not bind directly to the receptor but rather initiate a signaling cascade that causes CAR translocation from cytoplasm to nucleus and activation of nuclear CAR (Negishi et al., 2020).

Relative few CAR ligand agonists have been documented, and these agonists sometimes show marked species differences. For example, 1,4-bis-[2-(3,5-dichloropyridyloxy)]benzene is a potent agonist of mouse but not human CAR (Poland et al., 1980; Poland et al., 1981; Moore et al., 2000; Tzamei et al., 2000), while 6-(4-chlorophenyl)imidazo[2,1-b][1,3]thiazole-5-carbaldehyde O-(3,4-dichlorobenzyl)oxime (CITCO) is a potent agonist of human but not mouse CAR (Maglich et al., 2003; Zhang et al., 2013).

While PXR and CAR are xenobiotic-sensing receptors, endogenous activators of each receptor have been described. For example, the secondary bile acid lithocholic acid is an activator of PXR (Staudinger et al., 2001; Xie et al., 2001). We have studied the effects of inhibitors of the cholesterol biosynthetic pathway on cytochrome P450 (P450) expression in rodent and human hepatocytes (Kocarek et al., 1993; Kocarek and Reddy, 1996; Kocarek et al., 1998; Kocarek et al., 2002; Kocarek and Mercer-Haines, 2002; Shenoy et al., 2004; Jackson and Kocarek, 2008; Duniec-Dmuchowski et al., 2009; Pant and Kocarek, 2016; Rondini et al., 2016a; Rondini et al., 2016b). Use of these inhibitors has enabled the identification of metabolites in the pathway that function as endogenous modulators of CAR and PXR. For example, inhibition of 2,3-oxidosqualene:lanosterol cyclase, which converts squalene 2,3-oxide

to lanosterol, the first sterol in the pathway, causes accumulation of squalene 2,3;22,23-dioxide, which is a PXR ligand agonist (Shenoy et al., 2004; Duniec-Dmuchowski et al., 2009). By comparison, inhibition of squalene synthase, which catalyzes the first committed step in sterol biosynthesis (two steps upstream from 2,3-oxidosqualene:lanosterol cyclase), with squalestatin 1 (Squal1) induces CYP2B in rat liver and primary cultured rat hepatocytes (Kocarek et al., 1998). Squal1-mediated CYP2B induction proceeds through accumulation of the squalene synthase substrate farnesyl pyrophosphate (FPP), dephosphorylation of FPP to farnesol, and CAR activation (Kocarek and Mercer-Haines, 2002; Pant and Kocarek, 2016). Squal1-mediated CYP2B induction can be prevented by co-treatment with an upstream inhibitor in the cholesterol biosynthetic pathway, such as the HMG-CoA reductase (HMGCR) inhibitor pravastatin (Prava), and statin-mediated attenuation can be overcome by co-treatment with mevalonate (MVA), the product of HMGCR (Kocarek and Mercer-Haines, 2002). Co-treatment with alendronate, which inhibits the step immediately preceding squalene synthase (i.e., the condensation of geranyl pyrophosphate with isopentenyl pyrophosphate, catalyzed by farnesyl diphosphate synthase), also blocks Squal1-mediated CYP2B1 induction (Jackson and Kocarek, 2008).

Since cholesterol synthesis inhibitor treatments reduce cellular cholesterol levels, they activate the cell's mechanism for maintaining cholesterol homeostasis, which is mediated through the sterol regulatory element binding protein (SREBP) class of transcription factors. There are three SREBPs, SREBP1a, 1c, and 2. SREBP1a and SREBP1c are isoforms produced by alternative promoter usage and splicing from a single gene, SREBF1 (Horton et al., 2002; Osborne and Espenshade, 2009). Compared to SREBP1c, SREBP1a has a longer N-terminal region and stronger transactivation activity (Shimano et al., 1997), but SREBP1c is the predominant isoform that is expressed in liver where it regulates genes involved in fatty acid and triglyceride biosynthesis (Shimomura et al., 1997; Horton et al., 2002). By contrast, activation of SREBP2, transcribed from the SREBF2 gene, up-regulates many of the genes that encode

cholesterol biosynthesis enzymes as well as low density lipoprotein receptor, which increases cholesterol uptake into the cell (Horton et al., 2002).

Therefore, Squal1-mediated inhibition of squalene synthase exerts at least two major effects on hepatic gene expression – one that is mediated through inhibition of cholesterol biosynthesis and activation of SREBPs and one that is mediated through accumulation of an endogenous isoprenoid(s) and activation of CAR. In rat hepatocytes, these effects appear to occur with little cross-interference (Kocarek and Mercer-Haines, 2002; Jackson and Kocarek, 2008).

The initial goal of this study was to determine the ability of Squal1 to activate CAR in human hepatic systems, including primary cultured human hepatocytes, human hepatocytes *in vivo*, and differentiated HepaRG cells. Our findings indicate that, in contrast to rat, Squal1 has little ability to activate CAR in human hepatocytes, and suggest that this species difference is at least partially attributable to interference of an SREBP(s) with human CAR.



## Methods

**Materials.** Amphotericin B, bupropion hydrochloride, CITCO, dimethyl sulfoxide (DMSO), fatty acid-free bovine serum albumin (BSA), R-mevalonolactone, PB, rifampicin (Rif), tetradeuterated 1'-hydroxymidazolam, *trans*, *trans*-farnesol, and triamcinolone acetonide were purchased from Sigma-Aldrich (St. Louis, MO). Midazolam (certified reference material) was purchased from Caymen Chemical (Ann Arbor, MI). Doxycycline was purchased from Takara Bio (Mountain View, CA). Squalestatin 1, (E)-N-ethyl-6,6-dimethyl-N-[[3-[(4-thiophen3-ylthiophen-2-yl)methoxy]phenyl]methyl]hept-2-en-4-yn-1-amine (NB-598), Prava, and zoledronic acid were gifts from GlaxoSmithKline (Research Triangle Park, NC), Banyu Pharmaceutical (Tokyo, Japan), Bristol-Myers Squibb Co. (Stamford, CT), and Novartis Pharma AG (Basel, Switzerland), respectively. Cell culture media, MEM Non-Essential Amino Acids Solution, Penicillin-Streptomycin Solution, and fetal bovine serum (FBS) were purchased from Thermo Fisher Scientific (Waltham, MA). Human recombinant insulin (Novolin R) was purchased from Novo Nordisk Pharmaceuticals, Inc. (Princeton, NJ). Matrigel Basement Membrane Matrix and Cell Recovery Solution were purchased from Corning (Tewksbury, MA). Oligonucleotides were purchased from Integrated DNA Technologies (Coralville, IA). Restriction endonucleases were purchased from New England Biolabs (Ipswich, MA). Stable isotope-labeled (SIL) peptides (SpikeTides™\_TQL) for 450- and cytochrome P450 oxidoreductase (POR)-targeted quantitative proteomic analysis were purchased from JPT Peptide Technologies GmbH (Berlin, Germany). 6-Hydroxybupropion and 1'-hydroxymidazolam were purchased from Ceriliant (Round Rock, TX), and hexadeuterated 6-hydroxybupropion was purchased from Toronto Research Chemicals (Toronto, Ontario, Canada). Sources of additional reagents are described below.

**Primary human hepatocyte culture.** Plated primary cultures of human hepatocytes were obtained from either Lonza, Inc. (Walkersville, MD) or the Liver Tissue and Cell Distribution System (University of Minnesota; National Institutes of Health Contract Number N01-DK-7-0004/HHSN267200700004C). The donor characteristics for the human hepatocyte preparations are shown in Supplemental Table 1. After hepatocyte preparation and overnight culture, the hepatocytes, in 6- or 12-well plates ( $\sim 1.8 - 2.2 \times 10^6$  cells/well or  $0.8 - 1.0 \times 10^6$  cells/well, respectively), were express-shipped to Wayne State University. Upon receipt, medium was replaced with Williams' Medium E supplemented with 0.25 U/ml insulin, 0.1  $\mu$ M triamcinolone acetonide, 100 U/ml penicillin, 100  $\mu$ g/ml streptomycin, and 2.5  $\mu$ g/ml amphotericin B, and the cells were placed in an incubator and maintained at 37°C under a humidified atmosphere of 95% air/5% CO<sub>2</sub>. The following day, medium was replaced with Williams' Medium E, supplemented as above but lacking amphotericin B and containing 200  $\mu$ g/ml Matrigel. The following day, treatments were begun with 0.1  $\mu$ M Squal1, 0.1  $\mu$ M CITCO, 10  $\mu$ M Rif, or 10  $\mu$ M Prava (with or without CITCO or Rif), as described in the legends to Figs. 1 and 4 and Supplemental Figs. 1 to 3. Concentrated stock solutions (1000-fold) of Squal1 and Prava were prepared in water and sterilized by filtration. Concentrated stock solutions (1000-fold) of CITCO and Rif were prepared in dimethyl sulfoxide (DMSO). Medium and treatments were renewed after 24 hours, and after 48 hours of treatment hepatocytes were harvested for preparation of total RNA or microsomal fractions, or were processed for measurement of bupropion or midazolam hydroxylase activity.

**HepaRG cell culture.** HepaRG cells were obtained from Biopredic International (Saint-Grégoire, France) under a material transfer agreement with INSERM-Transfert (Paris, France) and cultured essentially as described previously (Pant et al., 2019). HepaRG cells (at passage #3-4 following receipt) were plated at a density of 24,000 cells/cm<sup>2</sup> into 6-well plates, and

cultures were maintained in HepaRG growth medium consisting of Williams' Medium E supplemented with 10% FBS, 5 µg/ml insulin, 0.1 µM triamcinolone acetonide, 100 U/ml penicillin, and 100 µg/ml streptomycin for 14 days. The confluent cultures were then incubated in HepaRG differentiation medium 1 (HepaRG growth medium supplemented with 1% DMSO) for 48 hours followed by HepaRG differentiation medium 2 (HepaRG growth medium supplemented with 2% DMSO) for a further 14 days, with medium replacement every 2-3 days. After differentiation, cells were cultured in HepaRG growth medium containing 2% FBS for 72 hours, after which treatments were begun with 0.1 µM Squal1, 0.1 µM CITCO, 100 µM PB, 30 µM Rif, 10 mM MVA, 10 µM zoledronic acid, 0.1 µM NB-598, or Prava (10 µM or 0.1 to 30 µM; alone or with MVA, CITCO, PB, or Rif), as described in the legends to Figs. 1B, 5, and 6. Concentrated stock solutions of Squal1, Prava, CITCO, and Rif were prepared as described above. Stock solutions of MVA, PB, and zoledronic acid were prepared in water, and a stock solution of NB-598 was prepared in DMSO. Medium and treatments were renewed after 24 hours, and after 48 hours of treatment cells were harvested for preparation of total RNA.

**CAR knockdown HepaRG cells.** A panel of five MISSION shRNA Lentiviral Transduction Particles targeting human CAR (TRCN0000236502, TRCN0000236503, TRCN0000236504, TRCN0000236505, and TRCN0000236506) and MISSION pLKO.1-puro Non-Mammalian shRNA Control Transduction Particles (SHC002V) were purchased from Sigma-Aldrich (St. Louis, MO). HepaRG cells were plated in HepaRG growth medium into 6-well plates at a density of 24,000 cells/cm<sup>2</sup> and incubated for 48 hours to achieve 60–70% confluency. The cells were then separately transduced with each of the above-described lentiviral particles at a multiplicity of infection of ~2. After 6 hours, transduction medium was replaced with fresh growth medium. After 48 hours, cells were incubated for 9 days in growth medium containing 1 µg/ml puromycin. The stably transduced HepaRG cells were then differentiated by incubating them in HepaRG

differentiation medium containing 1 µg/ml puromycin for 14 days. To assess CAR knockdown by the five lentiviral constructs, transduced and differentiated cells were incubated for 48 hours with HepaRG treatment medium containing 0.1% DMSO or 0.1 µM CITCO, and CAR and CYP2B6 mRNA levels were measured. By this analysis, lentiviral construct TRCN0000236504 produced the largest magnitude of CAR knockdown relative to non-targeting control, and HepaRG cells transduced with that construct were used in subsequent experiments. For experiments, HepaRG cells expressing non-targeting shRNA (shNT) and CAR-targeting shRNA (shCAR) were cultured as described above (under HepaRG cell culture), except that culture medium always contained 1 µg/ml puromycin. Differentiated cultures were treated for 48 hours with medium alone or containing 0.1% DMSO, 0.1 µM CITCO, 0.1% ethanol (+ 0.7% fatty acid-free BSA), or 100 µM farnesol (dissolved in ethanol; complexed with BSA (Pant et al., 2019)) and then harvested for preparation of total RNA.

**HepaRG cells conditionally expressing active SREBP2.** A doxycycline-inducible lentiviral vector expressing the transcriptionally active region of human SREBP2 was prepared using the Lenti-X Tet-One Inducible Expression System (Takara Bio, Mountain View, CA). The sequence encoding the first 481 amino acids of human SREBP2 (NCBI NM\_004599) was prepared by polymerase chain reaction, using a plasmid template (SREBP2-pcDNA3.1, previously described in (Kocarek and Mercer-Haines, 2002)), PfuUltra HF DNA Polymerase (Agilent Technologies, Santa Clara, CA), and the following primers: Forward primer: 5'-  
GCGGAATTCGCCACCATGGACGACAGCGGCGAG-3' (the underscored and bold nucleotides indicate an EcoRI site and a Kozak consensus sequence, respectively); Reverse primer: 5'-  
GCGGGATCCTCATCACCGTGAGCGGTCTACCATGC-3' (the underscored and bold nucleotides represent a BamHI site and tandem translation stop codons, respectively). The SREBP2 PCR fragment was resolved on a 0.8% agarose gel, purified using the QIAEX II Gel

Extraction Kit (Qiagen, Germantown, MD), digested with EcoRI and BamHI, and ligated into the pLVX-TetOne-Puro Vector. The resulting SREBP2-pLVX plasmid was then co-transfected with the Lenti-X HTX packaging system into HEK293 cells according to the manufacturer's instructions (Takara Bio) and medium was collected after 48 hours as crude lentiviral stock. HepaRG cells were plated into 24-well plates and grown to confluency in HepaRG growth medium as described above, after which the medium was changed to transduction medium (400  $\mu$ l HepaRG growth medium plus 200  $\mu$ l lentivirus-containing medium) containing 4  $\mu$ g/ml polybrene. The following day, medium was changed to standard HepaRG growth medium, and the next day 1  $\mu$ g/ml puromycin was added to select for stably transduced cells. Thereafter, the SREBP2-HepaRG cells were used for experiments essentially as described above for parental HepaRG cells except that the culture media included 0.5  $\mu$ M puromycin during cell growth and differentiation. The cells were then incubated with medium alone or containing 25-100 ng/ml doxycycline (stock solutions in water) for 48 hours. During the last 24 hours, the cells were co-treated with either 0.1% DMSO or 0.1  $\mu$ M CITCO.

**HepG2 cell culture and transient transfection.** HepG2 cells were purchased from the American Type Culture Collection (Manassas, VA) and cultured in high glucose Dulbecco's modified Eagle's medium (DMEM) supplemented with 10% fetal bovine serum, non-essential amino acids, 100 U/ml penicillin and 100  $\mu$ g/ml streptomycin. A CYP2B6 firefly luciferase reporter plasmid containing both the proximal PB-responsive enhancer module and distal xenobiotic-responsive element of the human CYP2B6 gene (Wang et al., 2003) was generously provided by Dr. Thomas Chang (University of British Columbia; British Columbia, CA). An expression plasmid containing the full-length coding sequence for hCAR1 and empty vector control were gifts from Dr. Curtis Omiecinski (Pennsylvania State University; College Park, PA) (Auerbach et al., 2003). HepG2 cells were plated into 12 well plates at a density of 150,000 cells

per well. Forty eight hours later (~50% confluency), cells were transiently transfected with a premixed complex containing 3  $\mu$ l Lipofectamine 2000 (Thermo Fisher Scientific), CYP2B6 reporter plasmid (800 ng), an expression plasmid for one of the SREBPs (previously described in (Kocarek and Mercer-Haines, 2002)) or pcDNA3.1 empty vector control (5-100 ng), 1 ng pRL-CMV (Promega Corporation; Madison, WI) to normalize for differences in transfection efficiency among wells, and pBluescript II KS+ as needed to adjust total plasmid DNA content to 1  $\mu$ g, diluted in 0.2 ml Opti-MEM medium. Medium was replaced 5 hours after transfection and 24 hours later. Forty-eight hours after transfection, HepG2 cells were harvested for the measurement of luciferase activity (firefly and *Renilla*) using the Dual Luciferase Reporter Assay System (Promega Corporation) and a GloMax 96 luminometer (Promega Corporation). Each treatment was performed in triplicate, and the entire experiment was replicated twice.

**Mice with humanized livers.** Preparation and treatment of mice with livers containing  $\geq 70\%$  human hepatocytes were performed by Yecuris Corporation (Tualatin, OR). The study was conducted in three phases, with phases 1 and 2 performed using human hepatocytes from the same donor, and phase 3 performed using hepatocytes from a different donor. In each phase, 8 male FRG KO/C57BL6 mice were transplanted with human hepatocytes and allowed to expand to  $\geq 70\%$  of the total hepatocyte population in the mouse liver. Prior to beginning treatments, the chimeric mice had been off CuRx™ Nitisinone drinking water for  $\geq 25$  days and sulfamethoxazole/trimethoprim for  $\geq 3$  days. Human repopulation levels were validated by enzyme-linked immunosorbent assay for blood levels of human albumin 2-3 days prior to beginning treatments. Within each experimental phase, 2 mice per group were treated for 5 days by subcutaneous injection with normal saline or 2.5, 5, or 10 mg/kg Squal1. The day after the last injection, mice were euthanized and livers were harvested, frozen in liquid nitrogen, and shipped on dry ice to Wayne State University for analysis of gene expression.

**RT-qPCR.** Primary cultured human hepatocytes and HepaRG cells: Total RNA was prepared from individual wells (from 12-well plates) of primary cultured human hepatocytes or HepaRG cells using the PureLink RNA isolation kit (Ambion, Carlsbad, CA). cDNA was prepared using either the Omniscript RT Kit (Qiagen) or the High-Capacity RNA-to-cDNA Kit (Thermo Fisher Scientific). Relative mRNA levels were determined by RT-qPCR, using the TaqMan Gene Expression Assays (Thermo Fisher Scientific) shown in Supplemental Table 2, as previously described (Dubaisi et al., 2018). Human TATA binding protein was used as the endogenous control gene. Each assay was performed in duplicate, and the untreated or DMSO-treated control group was used as the reference sample. Relative fold changes were determined using the comparative cycle threshold ( $\Delta\Delta CT$ ) method.

Humanized mouse livers: RNA was prepared using the PureLink RNA isolation kit, cDNA prepared using the Omniscript RT Kit, and CYP2B6 and human HMGR mRNA levels measured using TaqMan Gene Expression Assays. A GUSB TaqMan Gene Expression Assay (Supplemental Table 2) was used to normalize the human gene expression data, since this assay did not cross react with the orthologous mouse sequence.

**Targeted quantitative proteomic analysis.** Hepatocytes from 3 wells per treatment group (from 6-well plates) were washed once with cold phosphate-buffered saline and harvested by scraping in Cell Recovery Solution and combining into a 15 ml tube. Tubes were placed on ice for 30 minutes with periodic inversion to dissolve the Matrigel. The cells were pelleted by centrifugation, 100  $\mu$ l cold homogenization buffer (10 mM potassium phosphate, 0.15 M potassium chloride, 1 mM dithiothreitol, 10% glycerol, pH 7.4) was added, and the cells transferred to polystyrene sonicating tubes. The cells were homogenized using a Qsonica (Newtown, CT) model Q500 sonicator equipped with cup horn assembly. The tubes were then

centrifuged for 20 minutes at 20,000xg, 4°C, and the supernatants centrifuged for 1 hour at 105,000xg, 4°C. The microsomal pellets were rinsed with cold microsome storage buffer (10 mM Tris-HCl, 1 mM ethylenediaminetetraacetic acid, 20% glycerol, pH 7.4), and then suspended in 25 µl cold microsome storage buffer. Protein concentrations were determined using the Pierce BCA Protein Assay Kit (Thermo Fisher Scientific). Twenty micrograms of each microsomal preparation was analyzed in duplicate by digesting with trypsin and employing SIL peptide standards for quantification and nanoLC-MS/MS for separation and detection as previously described (Fallon et al., 2016; Khatri et al., 2019). Briefly, samples were solubilized in sodium deoxycholate, reduced with dithiothreitol, denatured with heat, and the cysteines carbamidomethylated with iodoacetamide. SIL peptide standards were added (1 pmol of each), followed by 1 µg of trypsin solution to give a protein:trypsin ratio of 20:1. The SIL peptides contain a tryptic linker at the C-terminus that is used for their quantification at the time of production. The peptides therefore need to be added prior to digestion so that the linker is removed. Samples were digested overnight (20 hours) at 37°C. Following termination of the trypsin reaction with trifluoroacetic acid, a deoxycholate precipitate formed and the supernatant was processed by C18 solid phase extraction (SPE) (10 mg/mL polymeric reversed phase cartridges). The SPE eluate was evaporated and reconstituted in slightly modified mobile phase (2% acetonitrile rather than 1%) before injection of 0.2% of the digested sample onto the nanoLC-MS/MS system (nanoAcquity [Waters, Milford, MA] coupled to a SCIEX [Framingham, MA] QTRAP 5500). The mass spectrometer was operated in the multiple reaction monitoring (MRM) mode and the MRMs acquired for the proteotypic peptides employed in the analysis are shown in Supplemental Table 3. The peptides had been selected based on *in silico* assessment, crude peptide evaluation, and consultation with the literature (Wang et al., 2008; Ohtsuki et al., 2012; Khatri et al., 2019). Peaks were integrated using MultiQuant 2.0.2 software (SCIEX) and peak area ratios of endogenous peptide to SIL response, of two MRMs combined,



were used to calculate peptide concentrations (in units of pmol/mg protein) (Khatri et al., 2019). Where more than one peptide was available for a protein the peptide giving the highest concentration, and showing stability in the analysis, was used to report the P450 and POR concentrations. The reporting peptides are indicated in Supplemental Table 3.

**Bupropion and midazolam hydroxylase activity.** Primary human hepatocytes in 12-well plates were cultured as described above and treated for 48 hours with medium alone or containing 0.1% DMSO, 10  $\mu$ M Prava, 0.1  $\mu$ M CITCO, or CITCO + Prava (3 wells/treatment group). The plate containing the cells treated with medium alone was then placed on ice (zero time control), and the culture medium of all cells was replaced with 0.7 ml medium containing 50  $\mu$ M bupropion or 5  $\mu$ M midazolam. Aliquots (0.6 ml) of the bupropion- or midazolam-containing medium from the zero time control cells were then transferred to 1.5 ml microcentrifuge tubes and placed at 4°C. The rest of the cells were incubated at 37°C for 1 hour, after which 0.6 ml medium was collected from each of the wells and placed at 4°C. All media samples were then centrifuged briefly at 13,000 RPM to pellet any residual cells, and the supernatants were transferred to fresh tubes and stored at -80°C until analyzed for 6-hydroxybupropion or 1'-hydroxymidazolam levels. The remaining medium was aspirated from the cultured cells, and the cells were washed once with cold phosphate-buffered saline and scraped into 500  $\mu$ L of RIPA Lysis and Extraction Buffer (Thermo Fisher Scientific) containing Halt Protease and Phosphatase Inhibitor Cocktail (Thermo Fisher Scientific) and transferred to 1.5 ml tubes. The protein concentrations in the lysates were then determined using the Pierce BCA Protein Assay Kit. Samples were prepared for liquid chromatographic analysis by dilution of 500  $\mu$ l of supernatant into 490  $\mu$ l of methanol followed by addition of 10  $\mu$ l of a 10  $\mu$ g/ml solution of deuterated internal standard in methanol. 6-Hydroxybupropion or 1'-hydroxymidazolam was measured in media samples by LC-MSMS with a Shimadzu 8040 triple quadrupole connected

to a Nexera-X2 binary UPLC with a high-pressure switching valve installed in the 30°C oven. Mobile phase A was 0.1% formic acid water and mobile phase B was 0.1% formic acid methanol. The system was plumbed to allow for injection of 10 µl of sample at 0.5 ml/min onto a pretreatment column (Thermo Hypersil Gold aQ 12 µm x 20 mm x 2.1 mm) using 100% A to remove buffer. After 0.5 minutes, the valve was switched from flowing to waste, to flow onto an analytical column (Restek Force C18 1.8 µm x 50 mm x 2.1 mm with Trident 2 µm filter cartridge) with 20% B for 1 minute followed by corresponding chromatography and mass spectrometry.

6-Hydroxybupropion chromatography and mass spectrometry: The gradient was linearly increased from 20% to 100% B over 3 minutes followed by a washing and equilibration phase. Elution time was 3.5 minutes as monitored by the transitions of 256:139 (quantitation ion) and 256:167 (90% ratio, qualitative ion). The internal standard, hexadeuterated 6-hydroxybupropion, had the same transitions except the starting ion was 262.

1'-Hydroxymidazolam chromatography and mass spectrometry: The gradient was linearly increased from 20% to 75% over 3 minutes. Elution time was 4.1 minutes as monitored by the transitions of 342:203 (quantitative ion) and 342:324 (40% ratio, qualitative ion). The internal standard, tetradeuterated 1'-hydroxymidazolam, was monitored by the transitions of 346:203 (quantitation ion) and 346:328 (qualitative ion).

**Statistical analysis.** Experiments were replicated as described in the individual figure legends. Statistical tests were performed using GraphPad Prism, version 8 for Windows (GraphPad Software, San Diego, CA). Values from replicated experiments where the data in each experiment were normalized to the experiment's own control group (thereby eliminating the variance from the control group) were analyzed by one sample t-tests to determine whether means were significantly different from the theoretical value of 1. Groups were also compared

by one- or two-way analysis of variance (ANOVA) followed by Tukey's or Sidak's multiple comparison test (MCT) (the control group was excluded from the ANOVA if normalization resulted in no variance in that group).  $p < 0.05$  was considered significantly different. Curves were fit to concentration-response data and  $IC_{50}$  or  $EC_{50}$  values and 95% confidence intervals were calculated using the log(inhibitor) vs. response (three parameters) or the log(agonist) vs. response (three parameters) functions of Prism.

## Results

Squal1 treatment increases CYP2B expression in primary cultured rat hepatocytes and rat liver (Kocarek et al., 1998; Kocarek and Mercer-Haines, 2002). To evaluate the ability of Squal1 to increase CYP2B6 expression, six preparations of primary cultured human hepatocytes were treated for 48 hours with 0.1  $\mu\text{M}$  Squal1 or the human CAR agonist CITCO (0.1  $\mu\text{M}$ ) and CYP2B6 mRNA levels were measured (Fig. 1A). CITCO selectively activates human CAR at a concentration of 0.1  $\mu\text{M}$ , while concentrations of 1  $\mu\text{M}$  or higher increasingly activate PXR (Maglich et al., 2003; Lin et al., 2020). CITCO treatment significantly increased CYP2B6 mRNA levels in the human hepatocyte cultures, producing a mean increase of ~4.1-fold over DMSO-treated control. However, Squal1 treatment did not increase CYP2B6 mRNA levels, despite producing effective squalene synthase inhibition as indicated by the ~6.3-fold increase in the amount of HMGCR reductase mRNA that occurred in response to reduced cholesterol biosynthesis. Similar effects were seen in differentiated cultures of HepaRG cells, as CITCO treatment significantly increased CYP2B6 mRNA levels (~9.2-fold), while Squal1 treatment had no effect, despite producing a significant increase in HMGCR mRNA content (~1.9-fold, Fig. 1B).

To evaluate the effects of Squal1 treatment on CYP2B6 expression in human hepatocytes *in vivo*, mice with livers repopulated with human hepatocytes were treated for 5 days with Squal1, at doses of 2.5, 5, and 10 mg/kg (Fig. 2). Squal1 treatment produced a ~2-fold increase in CYP2B6 mRNA levels in the hepatocytes used for experimental phases 1 and 2 (as described in Methods) but did not increase CYP2B6 mRNA levels in the hepatocytes used for phase 3, despite increasing HMGCR expression. Overall, these results indicate that Squal1 is, at most, a weak inducer of CYP2B6 in human hepatocytes.

Squal1-mediated CYP2B induction in primary cultured rat hepatocytes begins with inhibition of squalene synthase and requires FPP dephosphorylation to farnesol (Kocarek and Mercer-Haines, 2002; Jackson and Kocarek, 2008; Pant et al., 2019). Consistent with this mechanism, direct treatment with farnesol causes CYP2B induction in primary cultured rat hepatocytes (Kocarek and Mercer-Haines, 2002), rat liver (Horn et al., 2005), and HepaRG cells (Pant et al., 2019). To determine the CAR-dependency of this effect in HepaRG cells, differentiated HepaRG cells expressing a non-targeting or a CAR-targeting shRNA (shNT and shCAR, respectively) were treated with 0.1  $\mu$ M CITCO or 100  $\mu$ M farnesol. CAR mRNA levels were significantly lower in the shCAR-HepaRG cells than in the shNT-HepaRG cells (Fig. 3A), and CITCO treatment did not increase CYP2B6 mRNA content in the shCAR cells (Fig. 3B), demonstrating effective CAR knockdown (Fig. 3). Farnesol treatment significantly increased CYP2B6 mRNA levels in the shNT cells (~1.7-fold), consistent with our finding in parental HepaRG cells (Pant et al., 2019), but did not increase CYP2B6 mRNA content in shCAR cells (Fig. 3C).

Since the major effect of Squal1 is to inhibit cholesterol biosynthesis, we considered the possibility that Squal1 treatment does not induce CYP2B6 in human hepatocytes or HepaRG cells because inhibition of cholesterol synthesis interferes with CAR activation. To test this possibility, we evaluated the effect of treating primary cultured human hepatocytes with a different inhibitor of cholesterol biosynthesis, Prava, on the CYP2B6 induction that was produced by the human CAR agonist CITCO. Prava is an HMGCR inhibitor that, unlike some statins, does not directly activate CAR directly (Kobayashi et al., 2005; Howe et al., 2011; Režen et al., 2017). Seven preparations of primary cultured human hepatocytes were treated with 0.1  $\mu$ M CITCO alone or in the presence of Prava, and the levels of CYP2B6 and HMGCR mRNA were measured (Fig. 4A). For comparison, the hepatocytes were treated with the PXR agonist Rif, with and without Prava, and CYP3A4 mRNA levels were measured. As expected,

treatment with Prava alone increased HMGCR mRNA levels (~3.7-fold) but did not increase CYP2B6 or CYP3A4 mRNA levels; rather, levels of these P450 mRNAs were significantly decreased. Also CITCO treatment increased CYP2B6 mRNA levels (~6.1-fold) while Rif treatment increased CYP3A4 mRNA levels (~18.0-fold). Treatment with CITCO alone did not affect HMGCR mRNA content, while Rif treatment decreased HMGCR mRNA levels (~59%). Co-treatment with Prava completely inhibited CITCO-mediated CYP2B6 induction and partially attenuated Rif-mediated CYP2B6 and CYP3A4 induction. The effects of these treatments were also determined on microsomal CYP2B6 and CYP3A4 protein levels, as measured by quantitative targeted proteomic analysis (Fig.4B), and comparable results were obtained to those for mRNA. Also, Prava treatment inhibited CITCO-mediated induction of the CYP2B6 marker activity, bupropion hydroxylase (Fig. 4C). Midazolam 1'-hydroxylase activity was also measured in the same hepatocyte preparation as a marker of CYP3A4 activity. CITCO treatment produced a small (~51%) increase in midazolam 1-hydroxylase activity, which was comparable to the CITCO-mediated changes in CYP3A4 mRNA and protein levels that were observed (~41% and ~98% increases, respectively). These CITCO-mediated effects were inhibited by Prava co-treatment (Fig. 4C).

The effects of CITCO, Rif, and Prava treatment were also determined on the mRNA levels of several other genes that have been implicated as CAR targets in primary cultured human hepatocytes (Maglich et al., 2003; Kandel et al., 2016), including CYPs 1A1, 1A2, 2A6, 2A7, 2C8 and 2C9 and 5'-aminolevulinic acid synthase 1 (ALAS1), the rate-limiting enzyme in heme biosynthesis. CYP2C19 expression was also evaluated, since this P450 has also been identified as a CAR target (Chen et al., 2003). POR expression was also evaluated, due to this enzyme's essential function in P450 enzyme activity. The data are shown in Supplemental Fig. 1. Substantial interexperimental variability among human hepatocyte culture preparations precluded demonstration of many significant effects. However, CITCO treatment produced a

mean CYP2A6 mRNA level that was ~3.5-fold greater than control, and this effect was abolished by Prava co-treatment. Rif treatment did not increase CYP2A6 mRNA content. CITCO treatment did not affect the mRNA level of any of the other evaluated genes, except for a decrease in POR mRNA levels. Rif treatment significantly increased the CYP2C8 mRNA level. Also, while CITCO treatment had no effect on CYP1A1 or 1A2 expression, Rif treatment produced a small (~4.5-fold) increase in CYP1A1 mRNA content, and treatment with Prava, alone or in combination with CITCO or Rif, increased the mRNA levels of both CYP1A1 (~8- to 39-fold) and 1A2 (~2- to 3-fold) (Supplemental Fig. 1).

The effects of the CITCO, Rif, and Prava treatments were also evaluated on the protein levels of several P450s and POR in human hepatocytes (Supplemental Fig. 2). As seen at the mRNA level, CITCO treatment increased CYP2A6 protein content (~2.3-fold), and co-treatment with Prava treatment inhibited the increase. Both CITCO and Rif treatment significantly increased CYP2C8 protein levels (~1.6- and 1.9-fold respectively), and Prava co-treatment inhibited the CITCO- but not the Rif-mediated increase. CYP2C19 appeared to display a comparable expression pattern to that of CYP2C8, although treatment effects were not significant. Also as seen at the mRNA level, treatment with Prava increased the amount of CYP1A2 protein (~1.4-fold), and this increase was not affected by CITCO co-treatment.

CAR has also been implicated in the regulation of genes involved in lipid and glucose metabolism (Ueda et al., 2002; Kodama et al., 2004; Roth et al., 2008a; Dong et al., 2009; Gao et al., 2009; Zhai et al., 2010; Lynch et al., 2014). We therefore evaluated the effects of CITCO, Rif, and Prava treatments on expression of several genes involved in lipid (ACACA, FASN, SCD, PNPL3) and glucose (G6PC, PCK1) metabolism, as well as on the CAR, SREBPF1, and SREBPF2 transcription factors (Supplemental Fig. 3). Both CITCO and Rif treatment decreased the mRNA levels of the ACACA and FASN lipid metabolism genes (decreases of ~39 to 48%), and co-treatment with Prava prevented the CITCO- or Rif-mediated decreases. A similar pattern

was seen for PNPLA3, although the CITCO-mediated decrease (~42%,  $p=0.08$ ) was not significant. Treatment with Prava alone increased SCD mRNA content ~1.8-fold, and CITCO- or Rif co-treatment did not attenuate the Prava-mediated increase. Treatment with Prava and Rif, alone or in combination, decreased the mRNA levels of the glucose metabolism genes, G6PC and PCK1 (~54 to 73%), while CITCO had less effect. This same pattern of effects was observed for CAR (NR1H3). Prava treatment decreased the mRNA level of SREBPF1 (~72%), and this decrease was not affected by co-treatment with CITCO or Rif. The treatments did not show a clear pattern of effects on SREBPF2 mRNA levels, although CITCO and Prava in combination produced a significant increase.

To determine whether inhibitors of other steps in cholesterol biosynthesis could also attenuate CAR-inducible gene expression, HepaRG cells were treated with Prava, zoledronic acid (FPP synthase inhibitor), Squal1 (squalene synthase inhibitor), or NB598 (squalene monooxygenase inhibitor), alone or in combination with CITCO, and effects on CYP2B6 and HMGCR mRNA levels were measured (Fig. 5). Each of the inhibitors effectively blocked cholesterol biosynthesis, as indicated by increases in HMGCR mRNA levels (Fig. 5A), and each of the inhibitors also attenuated CITCO-inducible CYP2B6 expression (Fig. 2B). Also, the effect of Prava on HMGCR expression was reversed by co-treatment with MVA, the product of HMGCR. Likewise, co-treatment with MVA partially reversed Prava's suppressive effect on CITCO-mediated CYP2B6 expression, restoring expression to approximately the level seen in cells treated with CITCO and MVA alone.

These findings suggested a close correspondence between inhibition of cholesterol biosynthesis and suppression of CAR activation. To evaluate this relationship further, the concentration-dependent effects of Prava were determined on HMGCR expression, CITCO-mediated CYP2B6 induction, PB-mediated CYP2B6 induction (as an alternative CAR-activating treatment), and Rif-mediated CYP3A4 induction (to assess Prava's effects on PXR activation)



(Fig. 6). Treatment with Prava alone increased HMGCR mRNA levels with an  $EC_{50}$  of 4.29  $\mu$ M, and co-treatment with CITCO or PB did not affect Prava's potency for HMG-CoA reductase induction (i.e.,  $EC_{50}$  values of 3.65 and 7.91  $\mu$ M for Prava + CITCO and Prava + PB, respectively, with overlapping 95% confidence intervals) (Fig. 6A), suggesting that CAR activation did not affect the mechanism by which Prava treatment increased HMGCR expression. Prava treatment suppressed both CITCO- and PB-mediated CYP2B6 induction with  $IC_{50}$ s that were comparable to the  $EC_{50}$ s for HMGCR induction, suggesting identities of mechanism (Fig. 6B), although the confidence interval for Prava-mediated inhibition of PB-inducible expression was large due to the variability in effect that occurred at 0.3 and 1  $\mu$ M Prava. Prava treatment had little effect on Rif-mediated CYP3A4 induction, indicating that inhibition of cholesterol synthesis had a stronger suppressive effect on CAR than on PXR (Fig. 6B).

Since inhibition of cholesterol biosynthesis upregulates genes that control cholesterol homeostasis by activating SREBPs, we tested the effects of the three SREBPs, SREBP1a, SREBP1c, and SREBP2, on human CAR activity. HepG2 cells were transiently co-transfected with 5-100 ng of a plasmid expressing the active form of an SREBP and a CAR-responsive luciferase reporter plasmid, in the absence or presence of 25 ng of a plasmid expressing human CAR (the CAR1 isoform (Auerbach et al., 2003)) (Fig. 7). CAR1 is constitutively active when transfected into HepG2 cells, so no CAR-activating treatment was employed. In cells not transfected with CAR1, neither SREBP1a nor SREBP2 had a significant effect on reporter activity, while 50 and 100 ng SREBP1c increased reporter activity. However, this increase was mainly attributable to a suppressive effect on expression of *Renilla* luciferase from the pRL-CMV plasmid that was used to normalize reporter activities together with a slight activating effect on the empty reporter plasmid (pGL3-Basic) that was used as backbone for the CYP2B6 PBREM/XREM-Luc reporter, rather than a true activating effect of SREBP1c on the CAR-

responsive elements of the reporter. Transfection with CAR1 produced the expected increase in CYP2B6 reporter activity (~12-fold), and co-transfection with each SREBP produced marked effects on the CAR-activated reporter activity. Transfection with SREBP1a produced only a concentration-dependent suppression of reporter activity, while the effects of SREBP1c and SREBP2 were more complex, with lower concentrations increasing reporter activity (relative to transfection with an equal amount of empty pcDNA3.1 expression vector) and higher amounts then suppressing reporter activity. These effects were especially pronounced for SREBP2, which did not produce any potentially confounding effects on CYP2B6 reporter activity in cells not transfected with CAR1.

To investigate the possibility that SREBP2 activation can interfere with CAR signaling further, HepaRG cells were engineered for doxycycline-inducible expression of active SREBP2. Differentiated cells were then treated with doxycycline (0, 25, 50, 75, or 100 ng/ml) to induce SREBP2 expression, followed by treatment with DMSO or CITCO (Fig. 8). Doxycycline treatment produced a concentration-dependent increase in SREBP2 expression, which was accompanied by a concentration-dependent increase in expression of the SREBP2 target gene, HMGCR. These effects were also accompanied by a concentration-dependent suppression of CITCO-inducible CYP2B6 mRNA expression. These results, together with the SREBP transfection data in HepG2 cells, indicate that SREBP2 can interfere with CAR activity.

## Discussion

The initial goal of this study was to determine whether Squal1, a potent and efficacious inducer of CYP2B in primary cultured rat hepatocytes and rat liver (Kocarek et al., 1998; Kocarek and Mercer-Haines, 2002), also induces CYP2B6 in human hepatocytes. Squal1 treatment did not increase CYP2B6 expression in primary cultured human hepatocytes or differentiated HepaRG cells and produced a small and inconsistent increase in CYP2B6 expression in humanized mouse livers. The lack of effect of Squal1 on CYP2B6 expression is not attributable to a species difference in its binding to CAR, since Squal1-mediated activation of rat CAR occurs indirectly through inhibition of its pharmacological target, squalene synthase. Nor is the inability of Squal1 to induce CYP2B6 due to an inability to inhibit human squalene synthase, since Squal1 treatment effectively increased HMGCR expression in the human hepatic systems, indicating effective reduction of hepatocellular cholesterol levels and SREBP2 activation. It is also not due to an inability of farnesol and/or a farnesoid metabolite to activate human CAR since direct treatment of HepaRG cells with farnesol increased CYP2B6 expression in a CAR-dependent manner. Finally, we previously reported that Squal1 treatment of primary cultured hepatocytes isolated from humanized CAR transgenic mice increased expression of Cyp2b10 (Rondini et al., 2016b), demonstrating that Squal1 is capable of activating human CAR in the context of a mouse hepatocyte. Altogether, these findings indicated that something about the human hepatocyte suppresses Squal1-mediated CAR activation, and our results indicate that this suppressive effect is mediated by one or more of the SREBPs.

The findings in support of this conclusion include the following: (1) Co-treatment of primary cultured human hepatocytes or HepaRG cells with Prava abolished CITCO-mediated CYP2B6 expression in primary cultured human hepatocytes and HepaRG cells. It is important to

note that although several statins are capable of activating PXR and/or CAR, Prava is not one of them (El-Sankary et al., 2001; Kocarek et al., 2002; Kobayashi et al., 2005; Howe et al., 2011; Korhonova et al., 2015). (2) Co-treatment of HepaRG cells with any of several compounds that inhibit different steps of cholesterol biosynthesis inhibited CITCO-mediated CYP2B6 induction. MVA co-treatment rescued the Prava-mediated inhibition of CITCO-inducible CYP2B6 expression, further indicating that the effects of the inhibitor treatments were due to decreased cholesterol biosynthesis. It is noteworthy that MVA co-treatment did not restore CYP2B6 mRNA to the level present in cells treated with CITCO alone, likely because MVA itself produced some suppression of CITCO-mediated CYP2B6 induction through its conversion to one or more downstream metabolites that are capable of decreasing CAR activity (e.g., potentially an inverse agonist). (3) Co-transfection of HepG2 cells with the transcriptionally active forms of SREBP1a, SREBP1c, or SREBP2 produced concentration-dependent effects on human CAR1 activity. The various SREBPs did not produce identical effects, however, as SREBP1c and SREBP2, but not SREBP1a, increased reporter activity at low concentrations. All three forms of the SREBPs then produced concentration-dependent reductions of CAR activity, with the reductions especially steep for SREBP2. (4) Doxycycline-inducible expression of the transcriptionally active form of SREBP2 both increased expression of an SREBP2-responsive target gene (HMGCR) and decreased CITCO-mediated induction of CYP2B6.

To broaden our assessment of cholesterol synthesis inhibition on CAR-regulated gene expression, we evaluated the effects of Prava treatment on CITCO-mediated regulation of several genes that have been implicated as CAR targets in primary cultured human hepatocytes. These genes included P450s as well as genes involved in lipid and glucose metabolism. CAR has been implicated in the negative regulation of several genes involved in lipid and glucose metabolism, although a recent study indicated that CAR negatively regulated gluconeogenesis but not lipogenic genes in human hepatocytes (Lynch et al., 2014). Like

CYP2B6, CYP2A6 and CYP2C8 were induced by CITCO treatment (for CYP2C8, this was only observed for protein), and Prava inhibited the increases. These three P450s exhibited some differential regulation by Rif treatment, in that CYP2B6 and CYP2C8 protein levels were increased by Rif treatment, while CYP2A6 levels were unaffected, suggesting that CYP2A6 might be a more selective target of CAR than of PXR than are CYP2B6 and CYP2C8. For the P450s that were induced by Rif treatment, Prava co-treatment did not fully attenuate the Rif-mediated increases. CITCO treatment significantly suppressed the expression of two fatty acid biosynthesis genes, ACACA and FASN, but had less-clear effects on the other genes that were evaluated, and Prava and/or Rif treatments also modified the expression of several of the genes. However, for the genes that were suppressed by CITCO treatment, Prava co-treatment reversed the suppression, and overall our findings suggested that for genes that are regulated by CAR but not SREBP (as indicated by modulation by CITCO but not Prava), Prava co-treatment attenuated the CITCO-mediated effects, while for genes that are regulated by SREBP but not CAR (as indicated by modulation by Prava but not CITCO), CITCO co-treatment had relatively little impact on the Prava-mediated effects.

Two previous studies evaluated interactions between SREBPs and CAR. Roth et al. evaluated the interaction between the SREBP1 isoforms and CAR or PXR under conditions that increased SREBP1 activity in primary cultured mouse and human hepatocytes and mouse liver (Roth et al., 2008b). Treatment of primary cultured mouse hepatocytes with the liver X receptor agonist T0901317 or insulin decreased PB-mediated induction of Cyp2b10 and Cyp3a11; transduction of primary cultured human hepatocytes with the active form of SREBP1a or SREBP1c attenuated PB-mediated induction of CYP2B6 and CYP3A4 mRNA; and feeding of mice with a high cholesterol diet decreased PB-mediated induction of CAR and PXR target genes. Mechanistically, the authors demonstrated that the SREBP1 proteins do not associate with the Cyp2b10 CAR-binding motif unless CAR is present, and that the ligand-binding

domains of CAR and PXR physically interact with SREBP1 and reduce the interaction of CAR or PXR with certain coactivators (e.g., nuclear receptor coactivator 1).

Roth et al. (Roth et al., 2008a) also described another mechanism of CAR/PXR and SREBP1 interplay that addressed the observation that CAR or PXR activation in mice reduced hepatic triglyceride levels. The reduced triglyceride levels were accompanied by increased hepatic expression of Insig-1. Since Insig-1 binds to and inhibits SREBP cleavage-activating protein, which is required for proteolytic activation of the SREBPs, increased Insig-1 expression following CAR or PXR activation provides a plausible mechanism for triglyceride reduction. Although most experiments were conducted in mice, the authors also showed that PB treatment increased Insig-1 and decreased SREBP1c mRNA levels in primary cultured human hepatocytes, suggesting that CAR activation could also decrease human SREBP1c activity. In the current study, we did not observe that CITCO or Rif treatment decreased SREBF1 or SREBF2 mRNA levels in primary cultured human hepatocytes or that CITCO treatment interfered with Prava-mediated up-regulation of HMGCR in primary cultured human hepatocytes or HepaRG cells.

Several studies have investigated interactions between SREBPs and other nuclear receptors, providing additional insights into mechanisms whereby SREBPs modulate nuclear receptor activity. For example, several studies showed that one or more SREBP isoforms suppressed hepatocyte nuclear factor 4 alpha (HNF4 $\alpha$ )-activated gene transcription by inhibiting the recruitment of a key coactivator(s), most commonly PPARG coactivator 1 alpha (PGC1 $\alpha$ ), to HNF4 $\alpha$ . (Yamamoto et al., 2004; Ponugoti et al., 2007; Inoue et al., 2011). The molecular mechanisms by which the SREBP1 and SREBP2 isoforms suppressed HNF4 $\alpha$ -activated gene transcription appeared to differ, however. Yamamoto et al., (Yamamoto et al., 2004) and Ponugoti et al. (Ponugoti et al., 2007) reported that the SREBP1 isoforms bound through their N-terminal transactivation domains to the ligand-binding domain of HNF4 $\alpha$ . By comparison,

Inoue et al. (Inoue et al., 2011) found that while SREBP2 could bind to HNF4 $\alpha$  when the two proteins were studied in isolation, SREBP2 did not bind to HNF4 $\alpha$  when HNF4 $\alpha$  was bound to its response element. Rather, SREBP2 bound to PGC1 $\alpha$ , which then prevented the coactivator from interacting with HNF4 $\alpha$ .

Miyata et al. (Miyata et al., 2014) reported an interaction between SREBP2 and farnesoid X receptor (FXR) in intestinal cells. These investigators found that overexpression of active SREBP2 in the LS174T human colorectal adenocarcinoma cell line decreased expression of the FXR-target gene FGF19 and suppressed FXR-mediated activation of FGF19 reporter constructs containing an intact FXR-retinoid X receptor-binding motif. The authors provided evidence that these effects were attributable to binding of SREBP2 to FXR, which decreased the ability of FXR-retinoid X receptor to bind to its response element.

Our data indicate that SREBPs and human CAR interact under another scenario besides those described above; namely when SREBPs are activated in response to cholesterol synthesis inhibition (model shown in Fig. 9). Our data further highlight species differences in the regulation of CAR by sterol synthesis inhibition, in that rat CAR does not appear to be sensitive to this mode of regulation (Kocarek and Mercer-Haines, 2002; Jackson and Kocarek, 2008). This might explain the ability of Squal1 to induce CYP2B in rat but not human hepatocytes and also suggests a potential drug-drug interaction. More than 35 million people in the United States are being treated with a statin (Fookes, 2018), raising the possibility that CAR activation in these people might be attenuated somewhat by the statin treatment.

## Acknowledgment

The authors thank the developers of the HepaRG cell line at the Institut National de la Santé et de la Recherche Médicale (INSERM) for providing us with the cell line; the Liver Tissue and Cell Distribution System (University of Minnesota; National Institutes of Health Contract Number N01-DK-7-0004/HHSN267200700004C) for providing preparations of primary cultured human hepatocytes; and Drs. Thomas Chang (University of British Columbia; British Columbia, CA) and Curtis Omiecinski (Pennsylvania State University; College Park, PA) for providing plasmid reagents that supported these studies.



## Authorship Contributions

Participated in research design: Cuko, Duniec-Dmuchowski, Rondini, Pant, Fallon, Wilson, Peraino, Smith, Kocarek

Conducted experiments: Cuko, Duniec-Dmuchowski, Rondini, Pant, Fallon, Wilson, Peraino

Contributed new reagents or analytic tools: Fallon, Wilson, Peraino, Westrick, Smith

Performed data analysis: Cuko, Duniec-Dmuchowski, Rondini, Pant, Fallon, Peraino, Kocarek

Wrote or contributed to the writing of the manuscript: Cuko, Duniec-Dmuchowski, Rondini, Pant, Fallon, Wilson, Peraino, Westrick, Smith, Kocarek

## References

- Auerbach SS, Ramsden R, Stoner MA, Verlinde C, Hassett C, and Omiecinski CJ (2003) Alternatively spliced isoforms of the human constitutive androstane receptor. *Nucleic Acids Res* **31**:3194-3207.
- Chen Y, Ferguson SS, Negishi M, and Goldstein JA (2003) Identification of constitutive androstane receptor and glucocorticoid receptor binding sites in the CYP2C19 promoter. *Mol Pharmacol* **64**:316-324.
- Dong B, Saha PK, Huang W, Chen W, Abu-Elheiga LA, Wakil SJ, Stevens RD, Ilkayeva O, Newgard CB, Chan L, and Moore DD (2009) Activation of nuclear receptor CAR ameliorates diabetes and fatty liver disease. *Proc Natl Acad Sci U S A* **106**:18831-18836.
- Dubaisi S, Barrett KG, Fang H, Guzman-Lepe J, Soto-Gutierrez A, Kocarek TA, and Runge-Morris M (2018) Regulation of Cytosolic Sulfotransferases in Models of Human Hepatocyte Development. *Drug Metab Dispos* **46**:1146-1156.
- Duniec-Dmuchowski Z, Fang HL, Strom SC, Ellis E, Runge-Morris M, and Kocarek TA (2009) Human pregnane X receptor activation and CYP3A4/CYP2B6 induction by 2,3-oxidosqualene:lanosterol cyclase inhibition. *Drug Metab Dispos* **37**:900-908.
- El-Sankary W, Gibson GG, Ayrton A, and Plant N (2001) Use of a reporter gene assay to predict and rank the potency and efficacy of CYP3A4 inducers. *Drug Metab Dispos* **29**:1499-1504.
- Fallon JK, Smith PC, Xia CQ, and Kim MS (2016) Quantification of Four Efflux Drug Transporters in Liver and Kidney Across Species Using Targeted Quantitative Proteomics by Isotope Dilution NanoLC-MS/MS. *Pharm Res* **33**:2280-2288.

Fookes C (2018) Statins for high cholesterol: Are the benefits worth the risk?

*Drugs.com*: <https://www.drugs.com/article/statins-benefits-and-risks.html>.

Gao J, He J, Zhai Y, Wada T, and Xie W (2009) The constitutive androstane receptor is an anti-obesity nuclear receptor that improves insulin sensitivity. *J Biol Chem* **284**:25984-25992.

Horton JD, Goldstein JL, and Brown MS (2002) SREBPs: activators of the complete program of cholesterol and fatty acid synthesis in the liver. *J Clin Invest* **109**:1125-1131.

Howe K, Sanat F, Thumser AE, Coleman T, and Plant N (2011) The statin class of HMG-CoA reductase inhibitors demonstrate differential activation of the nuclear receptors PXR, CAR and FXR, as well as their downstream target genes. *Xenobiotica* **41**:519-529.

Inoue S, Yoshinari K, Sugawara M, and Yamazoe Y (2011) Activated sterol regulatory element-binding protein-2 suppresses hepatocyte nuclear factor-4-mediated Cyp3a11 expression in mouse liver. *Mol Pharmacol* **79**:148-156.

Jackson NM and Kocarek TA (2008) Suppression of CYP2B induction by alendronate-mediated farnesyl diphosphate synthase inhibition in primary cultured rat hepatocytes. *Drug Metab Dispos* **36**:2030-2036.

Kandel BA, Thomas M, Winter S, Damm G, Seehofer D, Burk O, Schwab M, and Zanger UM (2016) Genomewide comparison of the inducible transcriptomes of nuclear receptors CAR, PXR and PPARalpha in primary human hepatocytes. *Biochim Biophys Acta* **1859**:1218-1227.

Khatri R, Fallon JK, Rementer RJB, Kulick NT, Lee CR, and Smith PC (2019) Targeted quantitative proteomic analysis of drug metabolizing enzymes and transporters by nano LC-MS/MS in the sandwich cultured human hepatocyte model. *J Pharmacol Toxicol Methods* **98**:106590.

- Kobayashi K, Yamanaka Y, Iwazaki N, Nakajo I, Hosokawa M, Negishi M, and Chiba K (2005) Identification of HMG-CoA reductase inhibitors as activators for human, mouse and rat constitutive androstane receptor. *Drug Metab Dispos* **33**:924-929.
- Kocarek TA, Dahn MS, Cai H, Strom SC, and Mercer-Haines NA (2002) Regulation of CYP2B6 and CYP3A expression by hydroxymethylglutaryl coenzyme A inhibitors in primary cultured human hepatocytes. *Drug Metab Dispos* **30**:1400-1405.
- Kocarek TA, Kraniak JM, and Reddy AB (1998) Regulation of rat hepatic cytochrome P450 expression by sterol biosynthesis inhibition: inhibitors of squalene synthase are potent inducers of CYP2B expression in primary cultured rat hepatocytes and rat liver. *Mol Pharmacol* **54**:474-484.
- Kocarek TA and Mercer-Haines NA (2002) Squalestatin 1-inducible expression of rat CYP2B: evidence that an endogenous isoprenoid is an activator of the constitutive androstane receptor. *Mol Pharmacol* **62**:1177-1186.
- Kocarek TA and Reddy AB (1996) Regulation of cytochrome P450 expression by inhibitors of hydroxymethylglutaryl-coenzyme A reductase in primary cultured rat hepatocytes and in rat liver. *Drug Metab Dispos* **24**:1197-1204.
- Kocarek TA, Schuetz EG, and Guzelian PS (1993) Regulation of phenobarbital-inducible cytochrome P450 2B1/2 mRNA by lovastatin and oxysterols in primary cultures of adult rat hepatocytes. *Toxicol Appl Pharmacol* **120**:298-307.
- Kodama S, Koike C, Negishi M, and Yamamoto Y (2004) Nuclear receptors CAR and PXR cross talk with FOXO1 to regulate genes that encode drug-metabolizing and gluconeogenic enzymes. *Mol Cell Biol* **24**:7931-7940.
- Korhonova M, Dorcakova A, and Dvorak Z (2015) Optical Isomers of Atorvastatin, Rosuvastatin and Fluvastatin Enantiospecifically Activate Pregnane X Receptor PXR and Induce CYP2A6, CYP2B6 and CYP3A4 in Human Hepatocytes. *PLoS One* **10**:e0137720.

- Lin W, Bwayi M, Wu J, Li Y, Chai SC, Huber AD, and Chen T (2020) CITCO Directly Binds to and Activates Human Pregnane X Receptor. *Mol Pharmacol* **97**:180-190.
- Lynch C, Pan Y, Li L, Heyward S, Moeller T, Swaan PW, and Wang H (2014) Activation of the constitutive androstane receptor inhibits gluconeogenesis without affecting lipogenesis or fatty acid synthesis in human hepatocytes. *Toxicol Appl Pharmacol* **279**:33-42.
- Maglich JM, Parks DJ, Moore LB, Collins JL, Goodwin B, Billin AN, Stoltz CA, Kliewer SA, Lambert MH, Willson TM, and Moore JT (2003) Identification of a novel human constitutive androstane receptor (CAR) agonist and its use in the identification of CAR target genes. *J Biol Chem* **278**:17277-17283.
- Miyata M, Hata T, Yamazoe Y, and Yoshinari K (2014) SREBP-2 negatively regulates FXR-dependent transcription of FGF19 in human intestinal cells. *Biochem Biophys Res Commun* **443**:477-482.
- Moore LB, Parks DJ, Jones SA, Bledsoe RK, Consler TG, Stimmel JB, Goodwin B, Liddle C, Blanchard SG, Willson TM, Collins JL, and Kliewer SA (2000) Orphan nuclear receptors constitutive androstane receptor and pregnane X receptor share xenobiotic and steroid ligands. *J Biol Chem* **275**:15122-15127.
- Negishi M, Kobayashi K, Sakuma T, and Sueyoshi T (2020) Nuclear receptor phosphorylation in xenobiotic signal transduction. *J Biol Chem*.
- Ohtsuki S, Schaefer O, Kawakami H, Inoue T, Liehner S, Saito A, Ishiguro N, Kishimoto W, Ludwig-Schwellinger E, Ebner T, and Terasaki T (2012) Simultaneous absolute protein quantification of transporters, cytochromes P450, and UDP-glucuronosyltransferases as a novel approach for the characterization of individual human liver: comparison with mRNA levels and activities. *Drug Metab Dispos* **40**:83-92.

- Osborne TF and Espenshade PJ (2009) Evolutionary conservation and adaptation in the mechanism that regulates SREBP action: what a long, strange tRIP it's been. *Genes Dev* **23**:2578-2591.
- Pant A and Kocarek TA (2016) Role of Phosphatidic Acid Phosphatase Domain Containing 2 in Squalestatin 1-Mediated Activation of the Constitutive Androstane Receptor in Primary Cultured Rat Hepatocytes. *Drug Metab Dispos* **44**:352-355.
- Pant A, Rondini EA, and Kocarek TA (2019) Farnesol induces fatty acid oxidation and decreases triglyceride accumulation in steatotic HepaRG cells. *Toxicol Appl Pharmacol* **365**:61-70.
- Poland A, Mak I, and Glover E (1981) Species differences in responsiveness to 1,4-bis[2-(3,5-dichloropyridyloxy)]-benzene, a potent phenobarbital-like inducer of microsomal monooxygenase activity. *Mol Pharmacol* **20**:442-450.
- Poland A, Mak I, Glover E, Boatman RJ, Ebetino FH, and Kende AS (1980) 1,4-Bis[2-(3,5-dichloropyridyloxy)]benzene, a potent phenobarbital-like inducer of microsomal monooxygenase activity. *Mol Pharmacol* **18**:571-580.
- Ponugoti B, Fang S, and Kemper JK (2007) Functional interaction of hepatic nuclear factor-4 and peroxisome proliferator-activated receptor-gamma coactivator 1alpha in CYP7A1 regulation is inhibited by a key lipogenic activator, sterol regulatory element-binding protein-1c. *Mol Endocrinol* **21**:2698-2712.
- Režen T, Hafner M, Kortagere S, Ekins S, Hodnik V, and Rozman D (2017) Rosuvastatin and Atorvastatin Are Ligands of the Human Constitutive Androstane Receptor/Retinoid X Receptor  $\alpha$  Complex. *Drug Metab Dispos* **45**:974-976.
- Rondini EA, Duniec-Dmuchowski Z, Cukovic D, Dombkowski AA, and Kocarek TA (2016a) Differential Regulation of Gene Expression by Cholesterol Biosynthesis Inhibitors That

- Reduce (Pravastatin) or Enhance (Squalestatin 1) Nonsterol Isoprenoid Levels in Primary Cultured Mouse and Rat Hepatocytes. *J Pharmacol Exp Ther* **358**:216-229.
- Rondini EA, Duniec-Dmuchowski Z, and Kocarek TA (2016b) Nonsterol Isoprenoids Activate Human Constitutive Androstane Receptor in an Isoform-Selective Manner in Primary Cultured Mouse Hepatocytes. *Drug Metab Dispos* **44**:595-604.
- Roth A, Looser R, Kaufmann M, Blattler SM, Rencurel F, Huang W, Moore DD, and Meyer UA (2008a) Regulatory cross-talk between drug metabolism and lipid homeostasis: constitutive androstane receptor and pregnane X receptor increase Insig-1 expression. *Mol Pharmacol* **73**:1282-1289.
- Roth A, Looser R, Kaufmann M, and Meyer UA (2008b) Sterol regulatory element binding protein 1 interacts with pregnane X receptor and constitutive androstane receptor and represses their target genes. *Pharmacogenet Genomics* **18**:325-337.
- Shenoy SD, Spencer TA, Mercer-Haines NA, Abdolalipour M, Wurster WL, Runge-Morris M, and Kocarek TA (2004) Induction of CYP3A by 2,3-oxidosqualene:lanosterol cyclase inhibitors is mediated by an endogenous squalene metabolite in primary cultured rat hepatocytes. *Mol Pharmacol* **65**:1302-1312.
- Shimano H, Horton JD, Shimomura I, Hammer RE, Brown MS, and Goldstein JL (1997) Isoform 1c of sterol regulatory element binding protein is less active than isoform 1a in livers of transgenic mice and in cultured cells. *J Clin Invest* **99**:846-854.
- Shimomura I, Shimano H, Horton JD, Goldstein JL, and Brown MS (1997) Differential expression of exons 1a and 1c in mRNAs for sterol regulatory element binding protein-1 in human and mouse organs and cultured cells. *J Clin Invest* **99**:838-845.
- Staudinger JL, Goodwin B, Jones SA, Hawkins-Brown D, MacKenzie KI, LaTour A, Liu Y, Klaassen CD, Brown KK, Reinhard J, Willson TM, Koller BH, and Kliewer SA (2001) The

- nuclear receptor PXR is a lithocholic acid sensor that protects against liver toxicity. *Proc Natl Acad Sci U S A* **98**:3369-3374.
- Tzamelis I, Pissios P, Schuetz EG, and Moore DD (2000) The xenobiotic compound 1,4-bis[2-(3,5-dichloropyridyloxy)]benzene is an agonist ligand for the nuclear receptor CAR. *Mol Cell Biol* **20**:2951-2958.
- Ueda A, Hamadeh HK, Webb HK, Yamamoto Y, Sueyoshi T, Afshari CA, Lehmann JM, and Negishi M (2002) Diverse roles of the nuclear orphan receptor CAR in regulating hepatic genes in response to phenobarbital. *Mol Pharmacol* **61**:1-6.
- Wang MZ, Wu JQ, Dennison JB, Bridges AS, Hall SD, Kornbluth S, Tidwell RR, Smith PC, Voyksner RD, Paine MF, and Hall JE (2008) A gel-free MS-based quantitative proteomic approach accurately measures cytochrome P450 protein concentrations in human liver microsomes. *Proteomics* **8**:4186-4196.
- Wang YM, Ong SS, Chai SC, and Chen T (2012) Role of CAR and PXR in xenobiotic sensing and metabolism. *Expert Opin Drug Metab Toxicol* **8**:803-817.
- Watkins RE, Maglich JM, Moore LB, Wisely GB, Noble SM, Davis-Searles PR, Lambert MH, Kliewer SA, and Redinbo MR (2003) 2.1 A crystal structure of human PXR in complex with the St. John's wort compound hyperforin. *Biochemistry* **42**:1430-1438.
- Xie W, Radominska-Pandya A, Shi Y, Simon CM, Nelson MC, Ong ES, Waxman DJ, and Evans RM (2001) An essential role for nuclear receptors SXR/PXR in detoxification of cholestatic bile acids. *Proc Natl Acad Sci U S A* **98**:3375-3380.
- Yamamoto T, Shimano H, Nakagawa Y, Ide T, Yahagi N, Matsuzaka T, Nakakuki M, Takahashi A, Suzuki H, Sone H, Toyoshima H, Sato R, and Yamada N (2004) SREBP-1 interacts with hepatocyte nuclear factor-4 alpha and interferes with PGC-1 recruitment to suppress hepatic gluconeogenic genes. *J Biol Chem* **279**:12027-12035.



Zhai Y, Wada T, Zhang B, Khadem S, Ren S, Kuruba R, Li S, and Xie W (2010) A functional cross-talk between liver X receptor- $\alpha$  and constitutive androstane receptor links lipogenesis and xenobiotic responses. *Mol Pharmacol* **78**:666-674.

Zhang YK, Lu H, and Klaassen CD (2013) Expression of human CAR splicing variants in BAC-transgenic mice. *Toxicol Sci* **132**:142-150.

## Footnotes

This work was supported by the National Institutes of Health National Heart, Lung, and Blood Institute [Grant HL050710] and National Institute of Environmental Health Sciences [Grant P30 ES020957].

None of the authors have any conflicts of interest with the material presented in this manuscript or any affiliations with or involvement (either competitive or amiable) in any organization or entity with a direct financial interest in the subject matter or materials discussed in the manuscript.

1. Current Address: Center for Molecular Medicine and Genetics, Wayne State University, Detroit, MI

2. Current Address: Division of Gastroenterology and Hepatology, Department of Internal Medicine, University of Michigan Medical School, Ann Arbor, MI

3. Current Address: Ambys Medicines Inc., South San Francisco, CA

## Figure Legends

**Fig. 1.** Effects of Squal1 treatment on CYP2B6 and HMGCR mRNA levels in primary cultured human hepatocytes and HepaRG cells. Six preparations of primary cultured human hepatocytes (A) and 6 batches of HepaRG cells (B) were incubated for 48 hours in medium alone (untreated control) or containing 0.1% DMSO (DMSO control), 0.1  $\mu$ M CITCO, or 0.1  $\mu$ M Squal1, after which cells were harvested and CYP2B6 and HMGCR mRNA levels were measured. For each preparation/batch of cells, the mRNA level for the CITCO treatment group was normalized to the mRNA level for the DMSO control group, and the Squal1 group was normalized to the untreated control group. The data are then presented as mean fold of control  $\pm$  SEM (n=6). \*Significantly different from the theoretical value of 1,  $p < 0.05$ ; \*\* $p < 0.01$ ; \*\*\* $p < 0.001$  by one-sample t-test.

**Fig. 2.** Effects of Squal1 treatment on CYP2B6 and HMGCR mRNA levels in mice with humanized livers. Mice with humanized livers were treated for 5 days with saline (control) or with 2.5, 5, or 10 mg/kg Squal1. Following treatment, livers were dissected and CYP2B6 and human HMGCR mRNA levels were measured. The data shown in the left-hand side of the figure are from two experimental phases (1 and 2), which were performed using the same batch of human hepatocytes, and the data shown in the right-hand side of the panel are from phase 3, which was performed using a different batch of human hepatocytes. Within each phase, the hepatic mRNA levels from the Squal1-treated mice were normalized to the mean control mRNA level. The data for the Squal1 treatment groups are then presented as mean fold of control  $\pm$  SEM (for phases 1 and 2, n=4, \*significantly different from the theoretical value of 1 by one-sample t-test,  $p < 0.05$ ) or  $\pm$  range (for phase 3, n=2, statistical analysis not performed).

**Fig. 3.** Effect of CAR knockdown on CITCO- and farnesol-inducible CYP2B6 mRNA levels in HepaRG cells. Differentiated HepaRG cells stably expressing a non-targeting shRNA (shNT) or CAR-targeting shRNA (shCAR) were (A) incubated for 48 hours with medium, (B) treated for 48 hours with 0.1% DMSO or 0.1  $\mu$ M CITCO, or (C) treated for 48 hours with 0.1% ethanol or 100  $\mu$ M farnesol and harvested for measurement of CAR (A) or CYP2B6 (B and C) mRNA levels. For each experiment, the mRNA levels of the experimental groups (black bars) were normalized to the corresponding control groups (white bars), and the data are presented as mean fold of control  $\pm$  SEM (n=4 batches of cells for A; n=3 for B and C). \*Significantly different from the theoretical value of 1,  $p < 0.05$ ; \*\* $p < 0.01$  by one-sample t-test.

**Fig. 4.** Effects of Prava on CITCO-mediated CYP2B6 induction and Rif-mediated CYP3A4 induction in primary cultured human hepatocytes. **A:** Seven preparations of primary cultured human hepatocytes were treated for 48 hours with 0.1% DMSO, 10  $\mu$ M Prava (DMSO added to bring DMSO concentration to 0.1% in all treatment groups), 0.1  $\mu$ M CITCO (alone or with Prava), or 10  $\mu$ M Rif (alone or with Prava) and harvested for measurement of CYP2B6, CYP3A4, and HMGCR mRNA levels. **B:** Three preparations of primary cultured human hepatocytes were treated as described for panel A and harvested for targeted measurement of microsomal CYP2B6 and CYP3A4 protein concentrations by nanoLC-MS/MS. SIL peptide standards employed in the measurement and MRMs acquired are shown in Supplemental Table 3. For each hepatocyte preparation, mRNA or protein levels for the various treatment groups were normalized to the level for the DMSO control group. The data are then presented as mean fold of control  $\pm$  SEM. \*Significantly different from the theoretical value of 1,  $p < 0.05$ ; \*\* $p < 0.01$ ; \*\*\* $p < 0.001$  by one-sample t-test. #Significantly different from the CITCO-treated group,  $p < 0.05$  by one-way ANOVA and Sidak's MCT. **C:** Primary cultured human hepatocytes were treated with DMSO, Prava, CITCO, or CITCO and Prava as described for panel A, after which they

were incubated with medium containing bupropion or midazolam as described in Materials and Methods. The medium samples were then collected and analyzed for concentrations of 6-hydroxybupropion or 1'-hydroxymidazolam. Data are from one human hepatocyte preparation and are shown as mean 6-hydroxybupropion or 1'-hydroxymidazolam concentration (nmol per mg cellular protein)  $\pm$  SD (n=3 wells of hepatocytes).<sup>#</sup>Significantly different from the CITCO-treated group, p<0.05; \*\*p<0.01 by one-way ANOVA and Tukey's MCT.

**Fig. 5.** Effects of sterol synthesis inhibitor treatments on HMGCR expression and CITCO-mediated CYP2B6 induction in HepaRG cells. HepaRG cells were incubated for 48 hours in medium alone or containing 0.1% DMSO, 0.1  $\mu$ M Squal1, 10 mM MVA, 10  $\mu$ M Prava, Prava and MVA, 10  $\mu$ M zoledronic acid, or 1  $\mu$ M NB598, each treatment alone or in combination with 0.1  $\mu$ M CITCO. Following treatment, the cells were harvested and HMGCR and CYP2B6 mRNA levels were measured. **A:** Effects of sterol synthesis inhibitor treatments on HMGCR reductase mRNA levels. For each batch of cells, the mRNA levels for the sterol synthesis inhibitor treatments were normalized to the untreated or DMSO control group as appropriate, and the data are then presented as mean fold of control  $\pm$  SEM (n=3 cell batches), except for the NB598 group where the data are presented as mean fold of control  $\pm$  range (n=2). \*Significantly different from the theoretical value of 1, p<0.05; \*\*p<0.01 by one-sample t-test. Groups not sharing a letter are significantly different from each other by one-way ANOVA and Tukey's MCT, p<0.05 (ANOVA did not include control or NB598 groups). **B:** Effects of the sterol synthesis inhibitor treatments in the presence of CITCO on CYP2B6 mRNA levels. Data are expressed as mean percentages of the CITCO-treated group  $\pm$  SEM (n=3), except for the CITCO and NB598 group (mean  $\pm$  range, n=2). Groups not sharing a letter are significantly different from each other by one-way ANOVA and Tukey's MCT, p<0.05 (ANOVA did not include NB-598 group).

**Fig. 6.** Concentration-dependent effects of Prava treatment on HMGCR expression and CYP2B6 and CYP3A4 induction in HepaRG cells. HepaRG cells were incubated for 48 hours in medium alone (untreated) or containing 0.1% DMSO, 0.1  $\mu$ M CITCO, 100  $\mu$ M PB, 30  $\mu$ M Rif, or 0.1 to 30  $\mu$ M Prava alone or in combination with CITCO, PB, or Rif. Following treatment, cells were harvested and CYP2B6, CYP3A4, and HMGCR mRNA levels were measured. **A:** Concentration-response curves for Prava-inducible HMGCR expression, alone or in the presence of CITCO or PB. Data are presented as fold-increases relative to the appropriate control group (i.e., untreated for Prava and Prava + PB; DMSO for Prava + CITCO)  $\pm$  SEM (n=3 cell batches). EC<sub>50</sub> values with 95% confidence intervals (CIs) are shown. **B:** Concentration-response curves for Prava-mediated inhibition of CITCO- or PB-mediated CYP2B6 induction or Rif-mediated CYP3A4 induction. Data are presented as mean percentages of the mRNA levels measured in the groups treated with CITCO, PB, or Rif alone  $\pm$  SEM (n=3). IC<sub>50</sub> values with 95% CIs are shown.

**Fig. 7.** Effects of SREBP co-transfection on human CAR1 activity. HepG2 cells were transiently co-transfected with 5 to 100 ng of plasmid expressing the transcriptionally active form of SREBP1a, SREBP1c, or SREBP2 (or with pcDNA3.1 as empty expression vector control) and a CAR-responsive luciferase reporter plasmid, alone or in combination with 25 ng of a plasmid expressing human CAR1. Forty-eight hours after transfection, cells were harvested for measurement of luciferase activities. Data are presented as mean  $\pm$  sd normalized (firefly/*Renilla*) luciferase activities relative to the activity measured in cells transfected with 5 ng pcDNA3.1 without CAR1 (n=6 wells per group, derived from combining data from two independent experiments each with triplicate transfections). \*Significantly different from the corresponding pcDNA3.1 or pcDNA3.1+hCAR1 group transfected with the same amount of plasmid, p<0.05; \*\*p<0.01; \*\*\*p<0.001. #Significantly different from group transfected with 5 ng

of the same expression plasmid,  $p < 0.5$ ;  $##p < 0.01$ ;  $###p < 0.001$  by two-way ANOVA and Tukey's MCT.

**Fig. 8.** Effects of doxycycline-inducible expression of SREBP2 on HMGCR and CITCO-inducible CYP2B6 expression in HepaRG cells. HepaRG cells engineered for doxycycline-inducible expression of active SREBP2 transcription factor were incubated for 48 hours in medium alone (0 ng/mg doxycycline) or containing 25 to 100 ng/ml doxycycline. During the last 24 hours of that 48-hour incubation, half of the cells receiving each concentration of doxycycline were co-treated with 0.1% DMSO (white bars) and the other half were co-treated with 0.1  $\mu$ M CITCO (black bars). Following treatment, cells were harvested and SREBP2, HMGCR, and CYP2B6 mRNA levels were measured. In each experiment, mRNA levels in the various treatment groups were normalized to levels in untreated cells. Data are presented as mean fold of the 0 ng/ml doxycycline + DMSO treatment group  $\pm$  SEM ( $n=3$  cell batches). \*Significantly different from the corresponding group treated with 0 ng/ml doxycycline and the same chemical (i.e., DMSO or CITCO),  $p < 0.05$ ; \*\* $p < 0.01$ ; \*\*\* $p < 0.001$  by two-way ANOVA and Tukey's MCT. #Significantly different from the corresponding DMSO-treated group that received the same amount of doxycycline,  $p < 0.05$ ; ## $p < 0.01$ ; ### $p < 0.001$  by two-way ANOVA and Sidak's MCT.

**Fig. 9.** Cholesterol biosynthetic pathway focusing on the mevalonate/isoprenoid portion and highlighting metabolites, enzyme inhibitor sites of action, and transcription factors that are relevant to this study. Cholesterol biosynthesis inhibitors are shown in italicized purple text and their corresponding target enzymes are shown in italicized brown text. Featured metabolites (MVA, FPP, and farnesol) and transcription factors (SREBP2 and CAR) are boxed. Green arrows represent activation and red T-shaped symbols represent inhibition. Under basal conditions, FPP is converted primarily to squalene, which is subsequently converted to

cholesterol, which inhibits the activation of SREBPs. FPP is also converted to such non-sterol isoprenoids as ubiquinone, dolichol, and dolichyl phosphate, but little FPP is dephosphorylated to farnesol under basal conditions. Inhibition of cholesterol biosynthesis with any of the indicated compounds reduces cellular cholesterol levels, which causes SREBP activation and up-regulation of many cholesterol biosynthetic pathway genes (indicated by the thick green arrow). Specific inhibition of squalene synthase (e.g., by Squal1) causes both decreased cholesterol biosynthesis (thereby activating SREBPs) and accumulation of FPP, much of which is dephosphorylated to farnesol, which is subsequently converted to progressively oxidized metabolites (i.e., farnesal, farnesoic acid, and several dicarboxylic acids). We propose that farnesol is an endogenous activator of both rat and human CAR. However, Squal1 treatment only causes activation of rat CAR because in human hepatocytes, the activated SREBPs exert a suppressive effect on CAR.



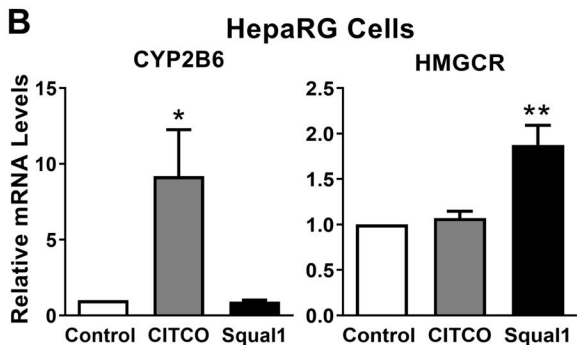
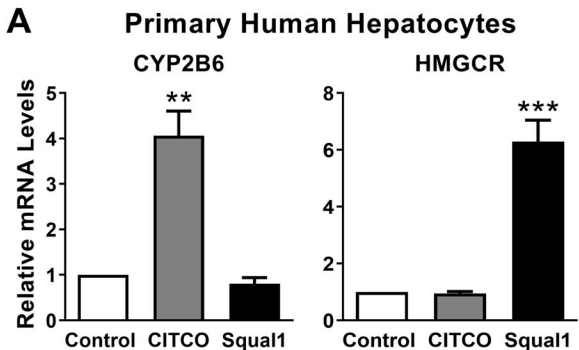
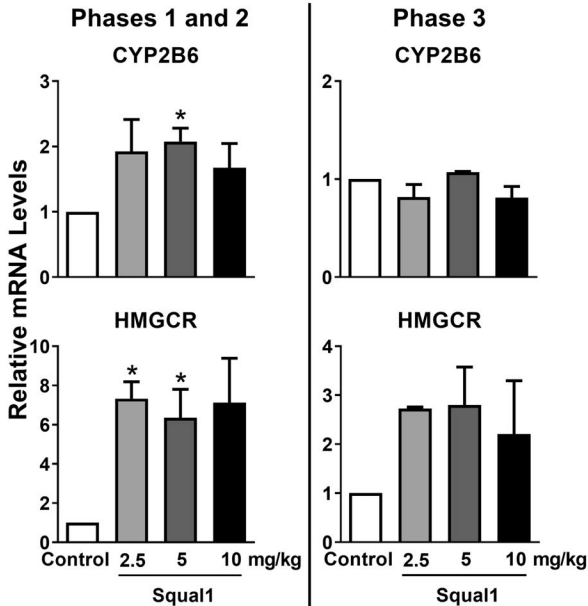


Figure 1



**Figure 2**

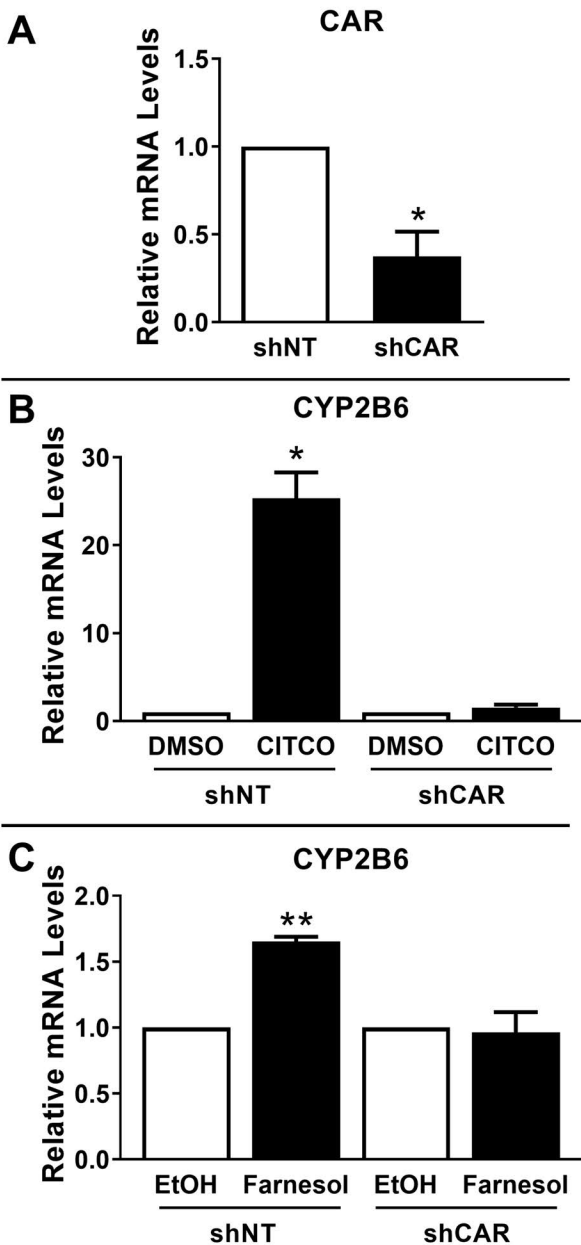


Figure 3

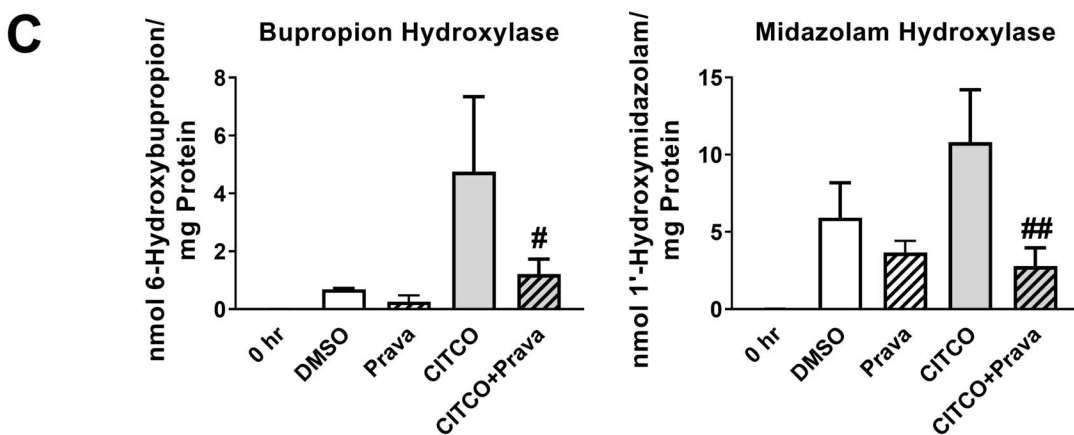
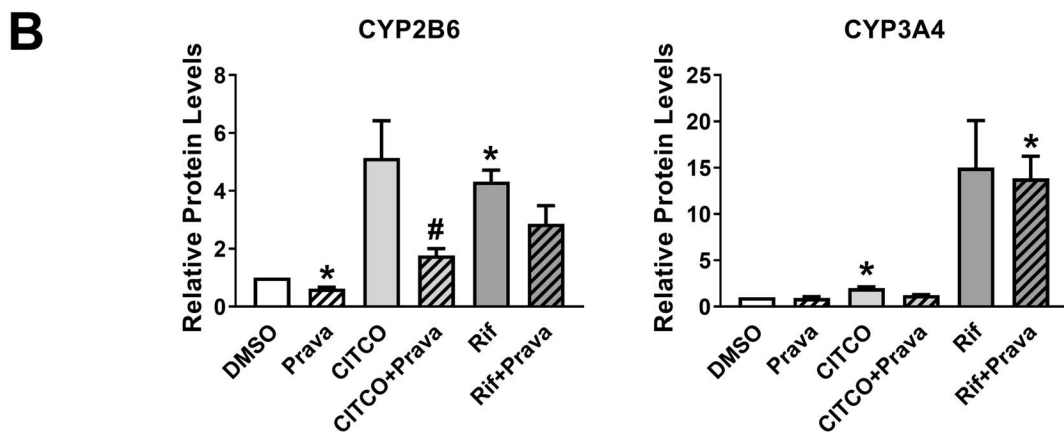
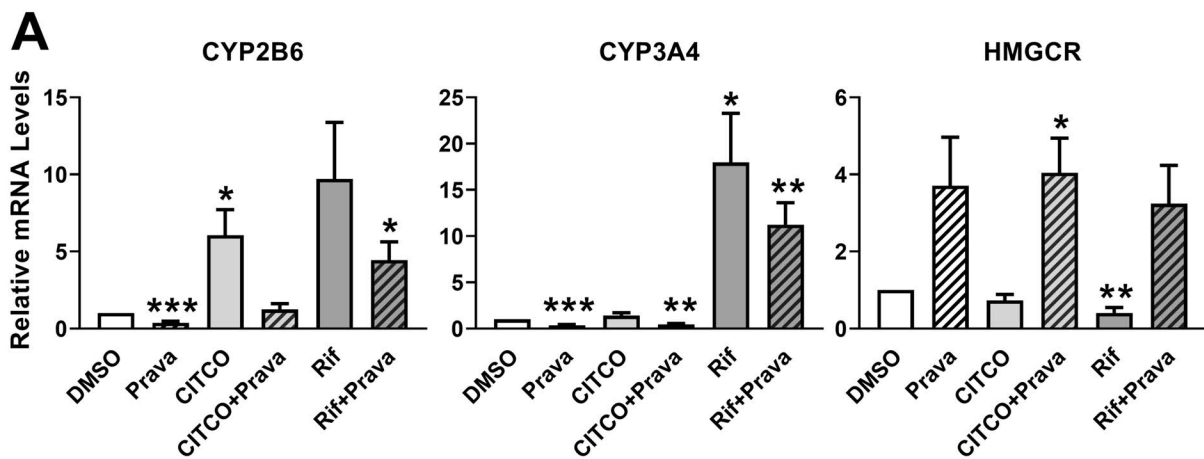


Figure 4

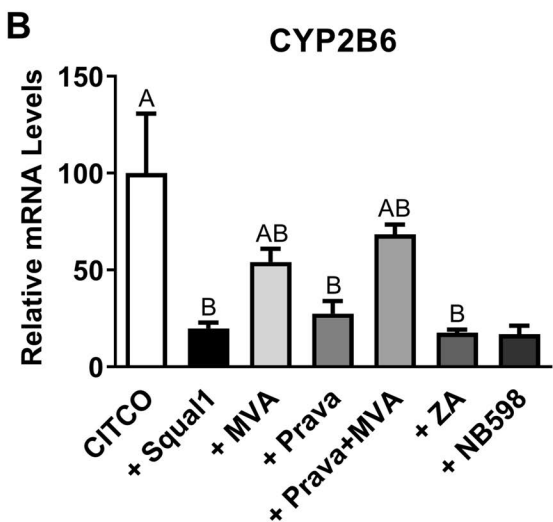
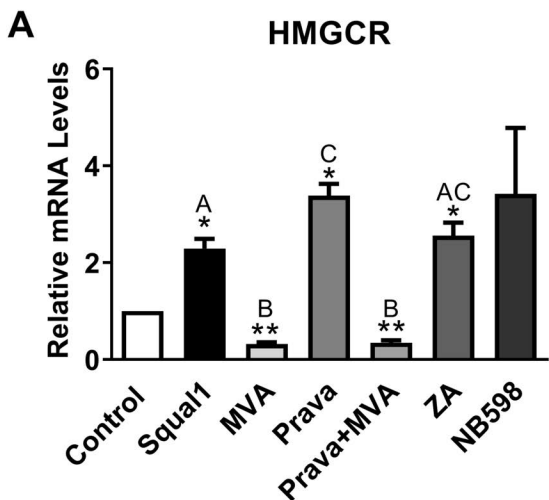
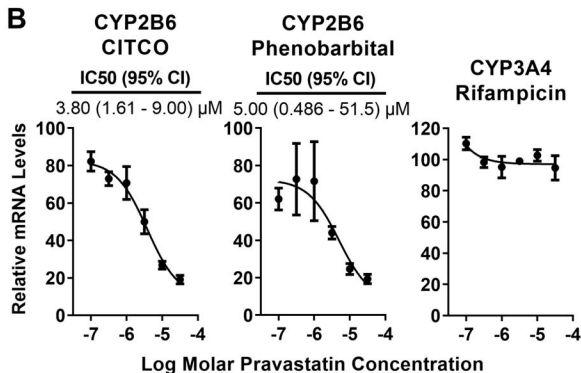
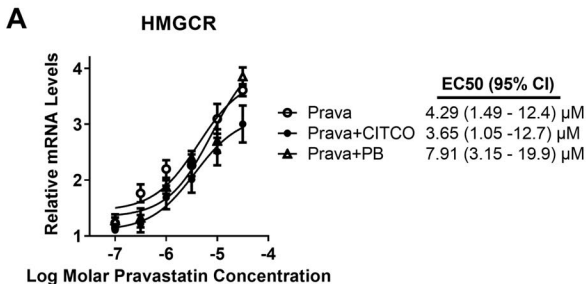


Figure 5



**Figure 6**

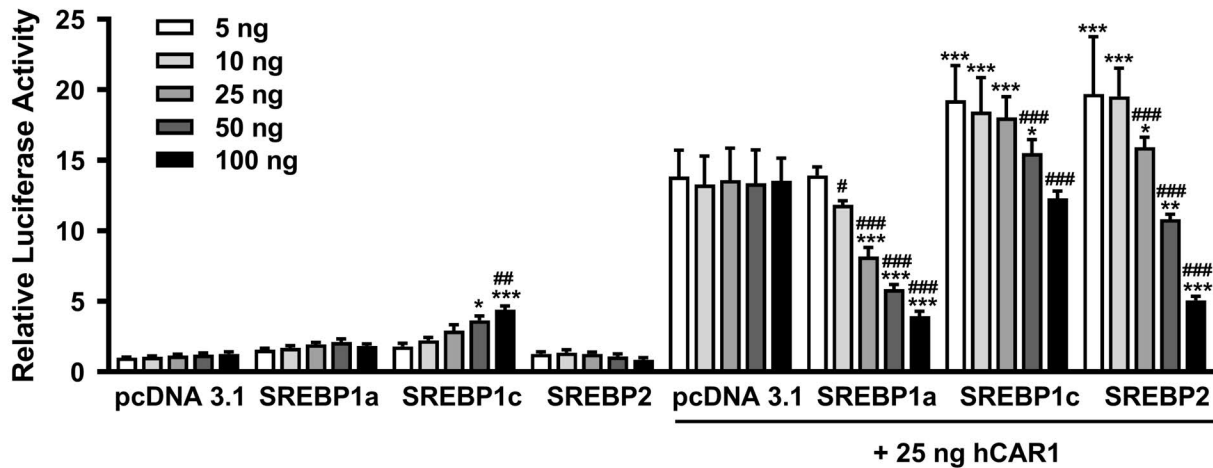


Figure 7

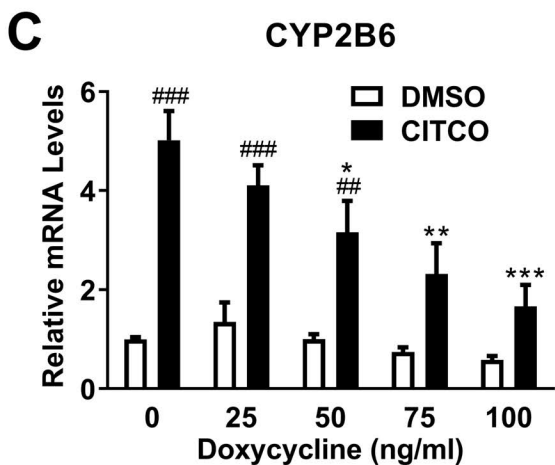
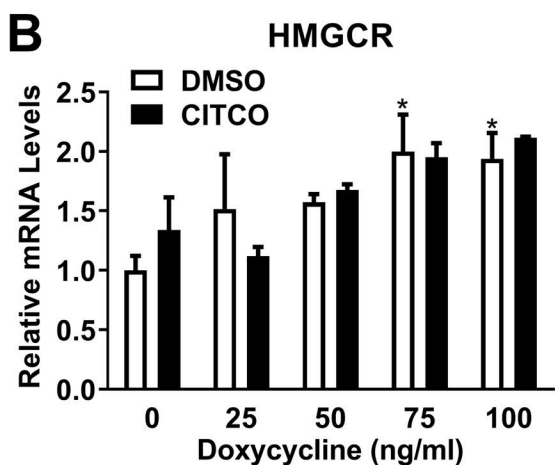
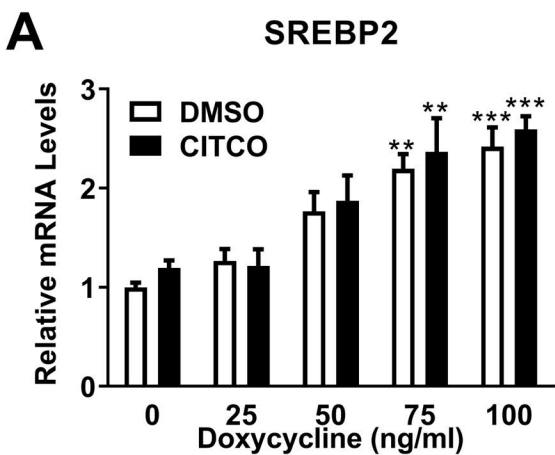


Figure 8



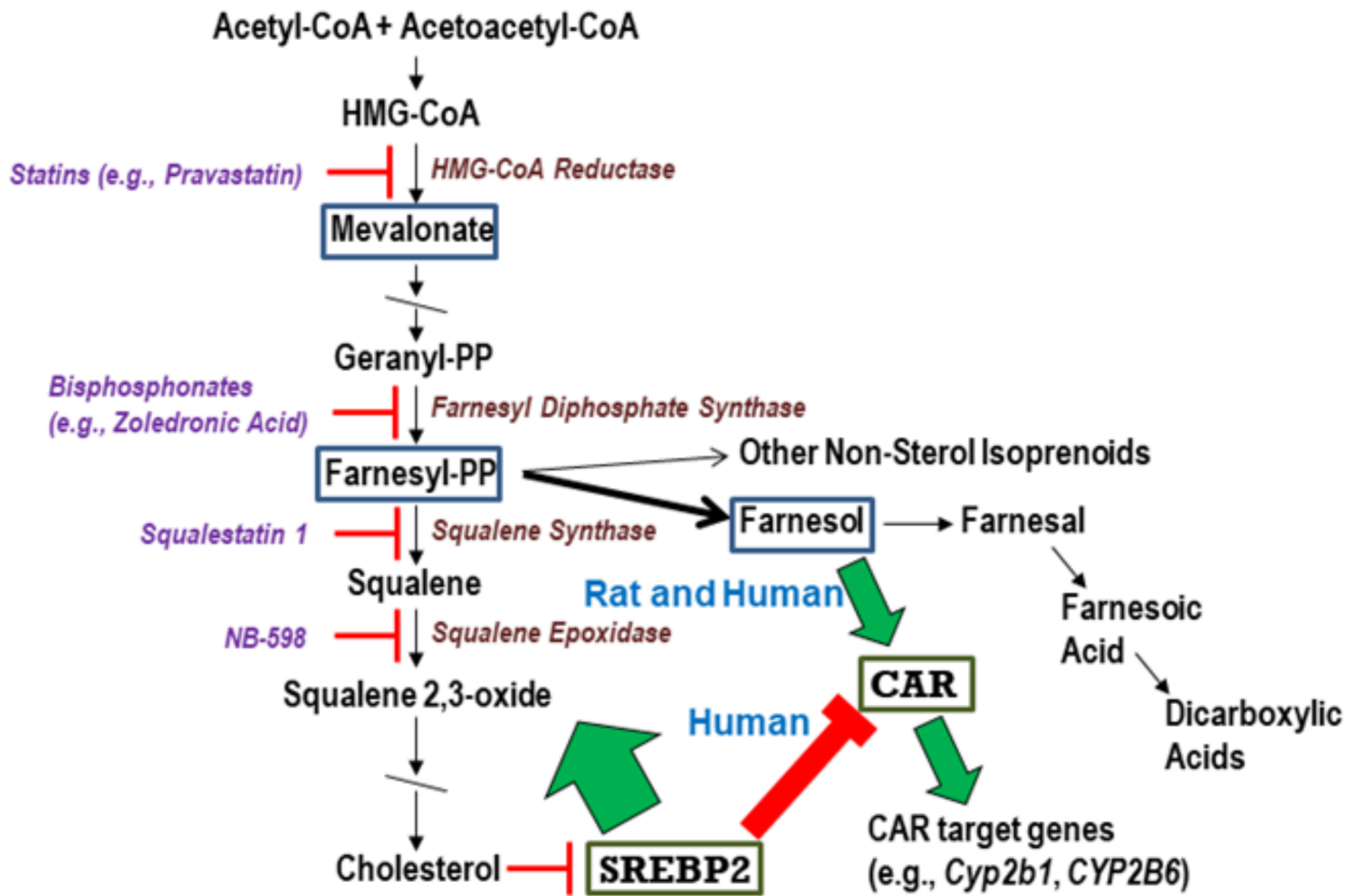


Figure 9

Liberta Cuko, Zofia Duniec-Dmuchowski, Elizabeth A. Rondini, Asmita Pant, John K. Fallon, Elizabeth M. Wilson, Nicholas J. Peraino, Judy A. Westrick, Philip C. Smith, and Thomas A. Kocarek. Negative Regulation of Human Hepatic Constitutive Androstane Receptor by Cholesterol Synthesis Inhibition: Role of Sterol Regulatory Element Binding Proteins. *Drug Metabolism and Disposition* DMD-AR-2020-000341.

**Supplemental Table 1. Donor age and sex for human hepatocyte preparations**

<b>Source</b>	<b>Identifier</b>	<b>Age (Years)</b>	<b>Sex</b>	<b>Data used for</b>
LTCDS	1938	49	Female	Fig. 1A
LTCDS	1967	25	Male	Fig. 1A
LTCDS	1975	56	Male	Fig. 1A
LTCDS	1987	50	Male	Fig. 1A
LTCDS	13-004	29	Female	Fig. 1A
LTCDS	14-005	39	Female	Fig. 1A
Yecuris	HHF07007	7	Female	Fig. 2 (Phases 1 and 2)
Yecuris	HHF17006	17	Female	Fig. 2 (Phase 3)
LTCDS	17-012	55	Male	Fig. 4A; Supplemental Figs. 1, 3
Lonza	HUM173391	56	Male	Fig. 4A; B; Supplemental Figs. 1, 2, 3
Lonza	HUM180671	57	Female	Fig. 4A; Supplemental Figs. 1, 3
Lonza	HUM180851	47	Male	Fig. 4A, B; Supplemental Figs. 1, 2, 3
Lonza	HUM181991	52	Female	Fig. 4A, B; Supplemental Figs. 1, 2, 3
Lonza	HUM191331	27	Female	Fig. 4A; Supplemental Figs. 1, 3
Lonza	HUM192291	51	Male	Fig. 4A, C; Supplemental Figs. 1, 3

LTCDS – Liver, Tissue, Cell Distribution Service

Liberta Cuko, Zofia Duniec-Dmuchowski, Elizabeth A. Rondini, Asmita Pant, John K. Fallon, Elizabeth M. Wilson, Nicholas J. Peraino, Judy A. Westrick, Philip C. Smith, and Thomas A. Kocarek. Negative Regulation of Human Hepatic Constitutive Androstane Receptor by Cholesterol Synthesis Inhibition: Role of Sterol Regulatory Element Binding Proteins. *Drug Metabolism and Disposition* DMD-AR-2020-000341.

**Supplemental Table 2. TaqMan Gene Expression Assays used for RT-qPCR**

<b>Gene Symbol</b>	<b>Gene Name</b>	<b>TaqMan Assay ID</b>
ACACA	Acetyl-CoA carboxylase alpha	Hs01046047_m1
ALAS1	5'-aminolevulinate synthase 1	Hs00963537_m1
CYP1A1	Cytochrome P450 1A1	Hs00153120_m1
CYP1A2	Cytochrome P450 1A2	Hs00167927_m1
CYP2A6	Cytochrome P450 2A6	Hs00868409_s1
CYP2A7	Cytochrome P450 2A7	Hs00751187_gH
CYP2B6	Cytochrome P450 2B6	Hs04183483_g1
CYP2C8	Cytochrome P450 2C8	Hs02383390_s1
CYP2C9	Cytochrome P450 2C9	Hs04260376_m1
CYP2C19	Cytochrome P450 2C19	Hs00426380_m1
CYP3A4	Cytochrome P450 3A4	Hs00604506_m1
FASN	Fatty acid synthase	Hs01005622_m1
G6PC	Glucose-6-phosphatase, catalytic	Hs02560787_s1
GUSB	Glucuronidase beta	Hs99999908_m1
HMGCR	3-Hydroxy-3-methylglutaryl-CoA reductase	Hs00168352_m1
NR1I3	Nuclear receptor 1I3 (CAR)	Hs00901571_m1
PCK1	Phosphoenolpyruvate carboxykinase 1	Hs00159918_m1
PNPLA3	Patatin like phospholipase domain containing 3	Hs00228747_m1
POR	Cytochrome p450 oxidoreductase	Hs01016332_m1
SCD	Stearoyl-CoA desaturase	Hs01682761_m1
SREBF1	Sterol regulatory element binding transcription factor 1	Hs01088679_g1
SREBF2	Sterol regulatory element binding transcription factor 2	Hs01081784_m1
TBP	TATA-box binding protein	Hs99999910_m1

Liberta Cuko, Zofia Duniec-Dmuchowski, Elizabeth A. Rondini, Asmita Pant, John K. Fallon, Elizabeth M. Wilson, Nicholas J. Peraino, Judy A. Westrick, Philip C. Smith, and Thomas A. Kocarek. Negative Regulation of Human Hepatic Constitutive Androstane Receptor by Cholesterol Synthesis Inhibition: Role of Sterol Regulatory Element Binding Proteins. *Drug Metabolism and Disposition* DMD-AR-2020-000341.

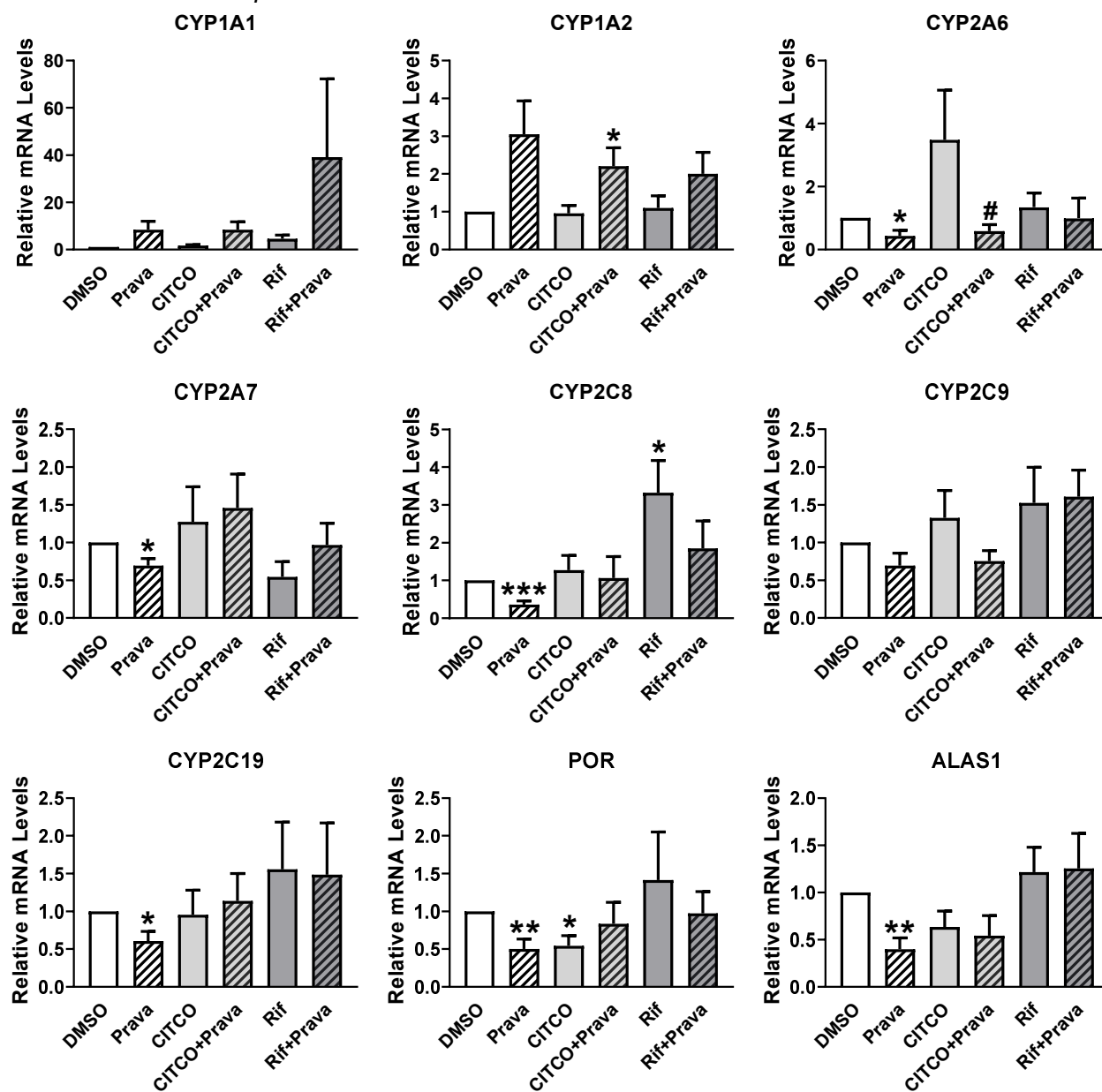
**Supplemental Table 3.** SIL proteotypic tryptic peptide standards and MRMs acquired for a set of human cytochromes 450 and cytochrome P450 oxidoreductase (POR). The peptides were purchased from JPT Peptide Technologies GmbH. Amino acids shown in bold (all C-terminus R or K) are <sup>13</sup>C and <sup>15</sup>N heavy labeled. The mass differences between labeled (shown) and unlabeled (not shown) R and K are 10 and 8, respectively. Mass shift for transition ions, between labeled and unlabeled, also depends on the charge state. The product ion for most of the heavy labeled peptide MRMs contains the heavy label. Peptide selection was based on *in silico* assessment, crude peptide evaluation and available literature (Wang et al., 2008; Ohtsuki et al, 2012; Khatri et al., 2019). Where necessary, peptides used for reporting concentrations are marked with ●.

UniProt Accession	Enzyme	Peptide Sequence	MRM1 <sup>a</sup> (Product Ion)	MRM2 (Product Ion)
P05177	CYP1A2	Y <sub>244</sub> LPNPALQR <sub>252</sub>	541.31/403.23 (y7)	541.31/594.36 (y5)
P11509	CYP2A6	G <sub>162</sub> TGGANIDPTFFLSR <sub>176</sub> ●	781.90/877.48 (y7)	781.90/992.51 (y8)
	CYP2A6	D <sub>401</sub> PSFFSNPQDFNPQHFLNEK <sub>420</sub>	806.04/811.40 (y13)	806.04/911.93 (y15)
P20813	CYP2B6	G <sub>110</sub> YGVIFANGNR <sub>120</sub>	589.30/801.42 (y7)	589.30/688.34 (y6)
	CYP2B6	E <sub>254</sub> TLDPSAPK <sub>262</sub>	483.26/507.31 (y5)	483.26/622.34 (y6)
	CYP2B6	G <sub>379</sub> YIIPK <sub>384</sub> ●	349.73/478.36 (y4)	349.73/365.27 (y3)
P10632	CYP2C8	N <sub>466</sub> LNTTAVTK <sub>474</sub>	485.28/742.43 (y7)	485.28/628.39 (y6)
P11712	CYP2C9	G <sub>98</sub> IFPLAER <sub>105</sub> ●	456.76/595.34 (y5)	456.76/298.18 (y5)
	CYP2C9	S <sub>460</sub> LVDPK <sub>465</sub>	333.70/252.18 (y2)	333.70/466.28 (y4)
P33261	CYP2C19	G <sub>98</sub> HFPLAER <sub>105</sub>	312.84/385.21 (y3)	312.84/439.21 (b4)
P10635	CYP2D6	S <sub>116</sub> QGVFLAR <sub>123</sub> ●	444.25/672.41 (y6)	444.25/516.32 (y4)
	CYP2D6	D <sub>381</sub> IEVQGFR <sub>388</sub>	487.25/745.39 (y6)	487.25/517.28 (y4)
P05181	CYP2E1	G <sub>113</sub> IIFNNGPTWK <sub>123</sub>	627.85/971.49 (y8)	627.85/824.42 (y7)
	CYP2E1	F <sub>360</sub> ITLVPSNLPHEATR <sub>374</sub> ●	568.98/566.29 (y10)	568.98/720.37 (y6)
P51589	CYP2J2	L <sub>214</sub> LDEVTYLEASK <sub>225</sub>	694.87/819.43 (y7)	694.87/918.50 (y8)
	CYP2J2	D <sub>276</sub> FIDAYLK <sub>283</sub> ●	496.76/730.42 (y6)	496.76/617.34 (y5)
P08684	CYP3A4	L <sub>331</sub> QEEIDAVLPNK <sub>342</sub>	688.88/366.22 (y3)	688.88/1135.61 (y10)
	CYP3A4	L <sub>477</sub> SLGGLLQPEKPVVLK <sub>492</sub> <sup>b</sup> ●	567.03/693.43 (y13)	567.03/664.92 (y12)
P20815	CYP3A5	D <sub>244</sub> TINFLSK <sub>251</sub>	473.30/217.10 (b2)	473.26/729.44 (y6)
P24462	CYP3A7	F <sub>213</sub> NPLDPFVLSIK <sub>224</sub>	699.41/568.85 (y10)	699.41/811.53 (y7)
	CYP3A7	E <sub>334</sub> IDTVLPNK <sub>342</sub> ●	518.80/366.23 (y3)	518.80/794.46 (y7)
	CYP3A7	F <sub>479</sub> GGLLLTEKPIVLK <sub>492</sub> <sup>b</sup>	512.66/694.96 (y13)	512.66/666.45 (y12)
P78329	CYP4F2	S <sub>109</sub> VINASAAIAPK <sub>120</sub> ●	575.35/850.50 (y9)	575.35/665.42 (y7)
	CYP4F2	F <sub>445</sub> DPENIK <sub>451</sub>	435.73/608.36 (y5)	435.73/304.68 (y5)
P16435	POR	F <sub>168</sub> AVFGLGNK <sub>176</sub>	480.78/643.38 (y6)	480.78/496.31 (y5)
	POR	G <sub>488</sub> VATNWLK <sub>495</sub> ●	463.76/770.42 (y6)	463.76/598.33 (y4)

<sup>a</sup> MRMs are roughly in order of highest intensity

<sup>b</sup> KP is not cleaved by trypsin. P prevents trypsin cleavage at the adjacent preceding K

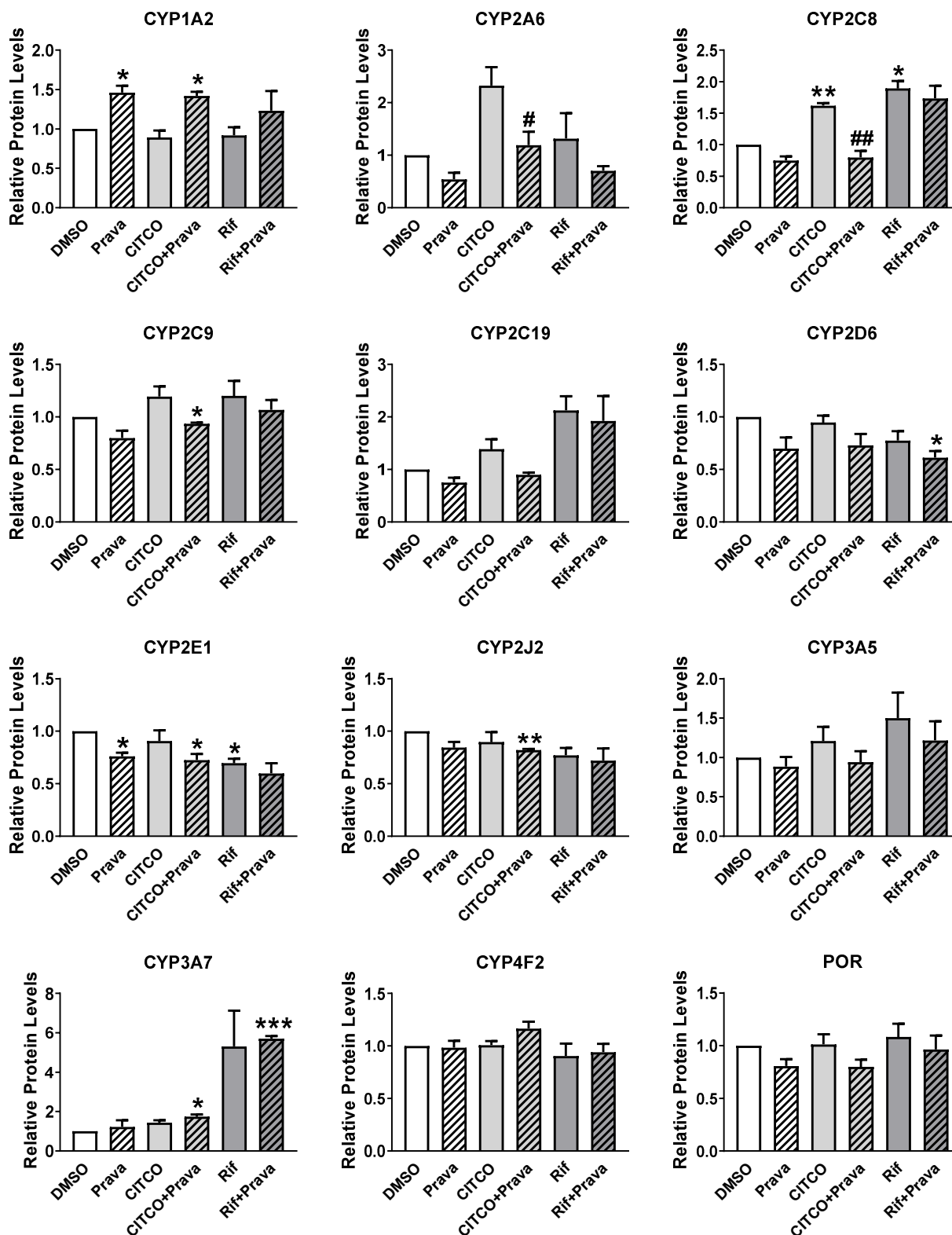
Liberta Cuko, Zofia Duniec-Dmuchowski, Elizabeth A. Rondini, Asmita Pant, John K. Fallon, Elizabeth M. Wilson, Nicholas J. Peraino, Judy A. Westrick, Philip C. Smith, and Thomas A. Kocarek. Negative Regulation of Human Hepatic Constitutive Androstane Receptor by Cholesterol Synthesis Inhibition: Role of Sterol Regulatory Element Binding Proteins. *Drug Metabolism and Disposition* DMD-AR-2020-000341.



**Supplemental Fig. 1.** Effects of Prava, CITCO, and Rif on levels of P450, POR, and ALAS1 mRNA in primary cultured human hepatocytes. Primary cultured human hepatocytes (5 to 7 hepatocyte preparations) were treated for 48 hours with 0.1% DMSO, 10  $\mu$ M Prava, 0.1  $\mu$ M CITCO (alone or with Prava), or 10  $\mu$ M Rif (alone or with Prava) and harvested for measurement of the indicated P450, POR, and ALAS1 mRNA levels. For each hepatocyte preparation, mRNA levels for the various treatment groups were normalized to the level for the DMSO control group. The data are then presented as mean fold of control  $\pm$  SEM (n=7 hepatocyte preparations for all genes except CYP1A1, where n=5). \*Significantly different from the theoretical value of 1,  $p < 0.05$ ; \*\* $p < 0.01$ ; \*\*\* $p < 0.001$  by one-sample t-test. #Significantly different from the CITCO-treated group,  $p < 0.05$  by one-way ANOVA and Sidak's multiple comparison test.

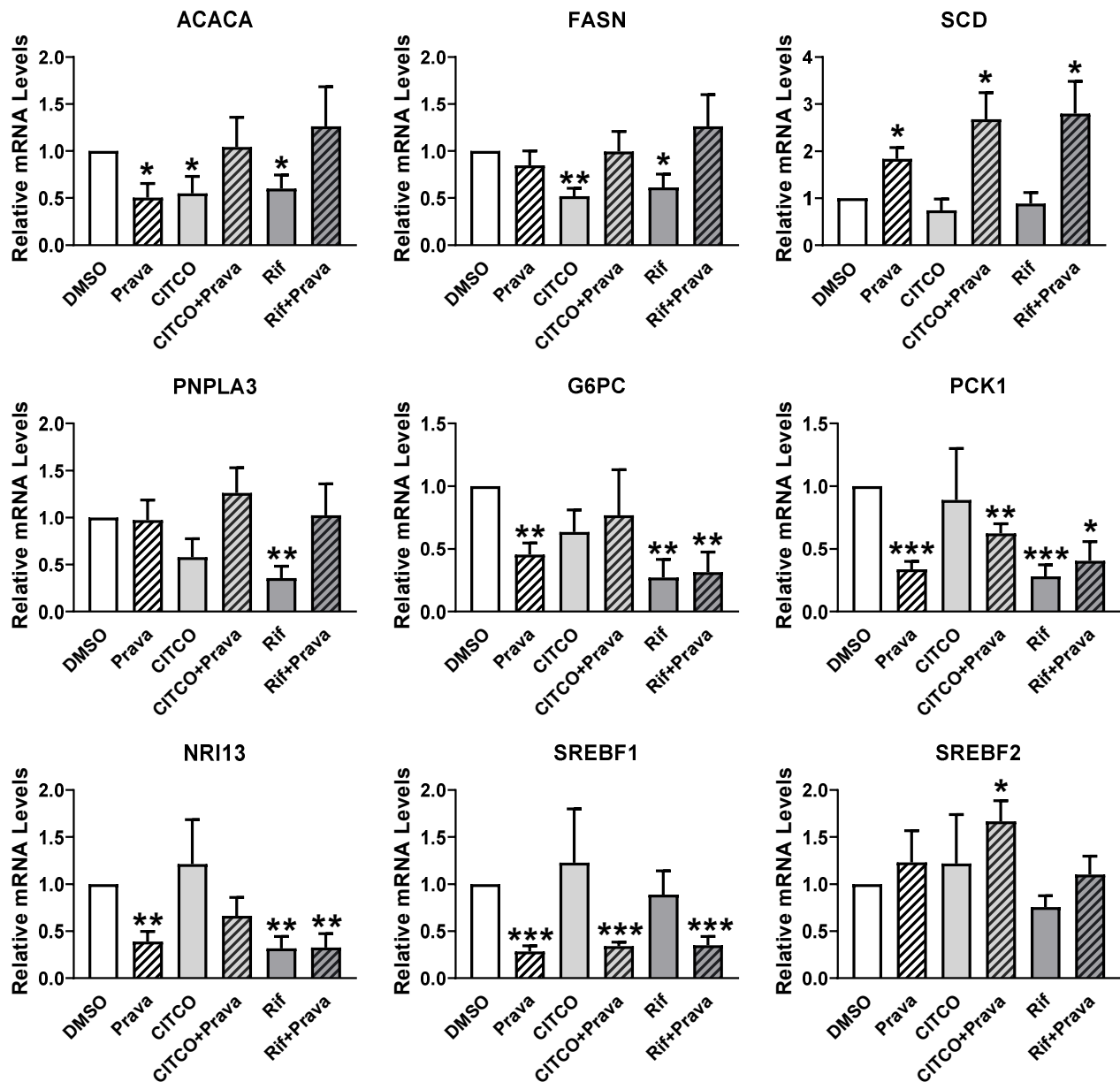
Liberta Cuko, Zofia Duniec-Dmuchowski, Elizabeth A. Rondini, Asmita Pant, John K. Fallon, Elizabeth M. Wilson, Nicholas J. Peraino, Judy A. Westrick, Philip C. Smith, and Thomas A. Kocarek. Negative Regulation of Human Hepatic Constitutive Androstane Receptor by Cholesterol Synthesis Inhibition: Role of Sterol Regulatory Element Binding Proteins. *Drug Metabolism and Disposition* DMD-AR-2020-000341.

## Supplemental Fig. 2



**Supplemental Fig. 2.** Effects of Prava, CITCO, and Rif on concentrations of P450 and POR protein in primary cultured human hepatocytes determined by nanoLC-MS/MS. SIL peptide standards employed and MRMs acquired are shown in Supplemental Table 3. Three preparations of primary cultured human hepatocytes were treated for 48 hours with 0.1% DMSO, 10  $\mu$ M Prava, 0.1  $\mu$ M CITCO (alone or with Prava), or 10  $\mu$ M Rif (alone or with Prava) and harvested for measurement of the indicated P450 and POR protein levels. For each hepatocyte preparation, protein levels for the various treatment groups were normalized to the level for the DMSO control group. The data are then presented as mean fold of control  $\pm$  SEM. \*Significantly different from the theoretical value of 1,  $p < 0.05$ ; \*\* $p < 0.01$ ; \*\*\* $p < 0.001$  by one-sample t-test. #Significantly different from the CITCO-treated group,  $p < 0.05$ ; ## $p < 0.01$  by one-way ANOVA and Sidak's multiple comparison test.

Liberta Cuko, Zofia Duniec-Dmuchowski, Elizabeth A. Rondini, Asmita Pant, John K. Fallon, Elizabeth M. Wilson, Nicholas J. Peraino, Judy A. Westrick, Philip C. Smith, and Thomas A. Kocarek. Negative Regulation of Human Hepatic Constitutive Androstane Receptor by Cholesterol Synthesis Inhibition: Role of Sterol Regulatory Element Binding Proteins. *Drug Metabolism and Disposition* DMD-AR-2020-000341.



**Supplemental Fig. 3.** Effects of Prava, CITCO, and Rif on mRNA levels of lipid and glucose metabolic genes, CAR (NR1I3), and SREBFs in primary cultured human hepatocytes. Primary cultured human hepatocytes (6 to 7 hepatocyte preparations) were treated for 48 hours with 0.1% DMSO, 10  $\mu$ M Prava, 0.1  $\mu$ M CITCO (alone or with Prava), or 10  $\mu$ M Rif (alone or with Prava) and harvested for measurement of the indicated mRNAs. For each hepatocyte preparation, mRNA levels for the various treatment groups were normalized to the level for the DMSO control group. The data are then presented as mean fold of control  $\pm$  SEM (n=7 hepatocyte preparations for ACACA, SCD, NR1I3, SREBF1, and SREBF2; n=6 hepatocyte preparations for FASN, PNPLA3, G6PC, and PCK1). \*Significantly different from the theoretical value of 1, p<0.05; \*\*p<0.01; \*\*\*p<0.001 by one-sample t-test.